AD-A116 663 GRUMMAN AEROSPACE CORP BETHPAGE NY RESEARCH DEPT F/G 11/6
FATIGUE BEHAVIOR OF SOLUTION TREATED AND QUENCHED TI-6AL-4V,(U)
MAY 81 J R KENNEDY N00019-78-C-0505
UNCLASSIFIED RE-630 NL

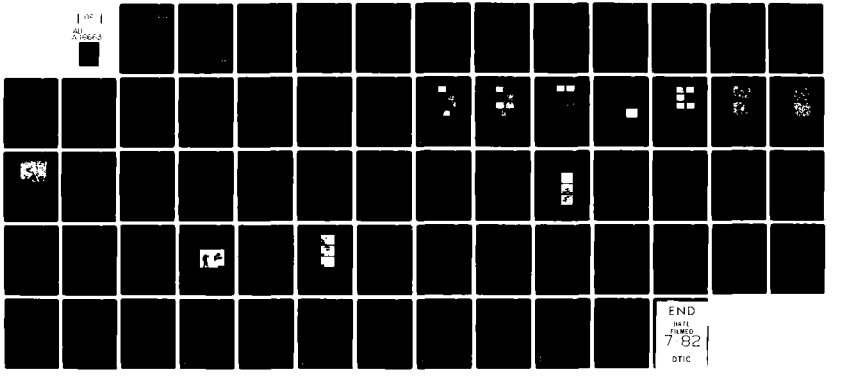

final report

FATIGUE BEHAVIOR OF SOLUTION TREATED AND QUENCHED TI-6AI-4V

Prepared Under Contract N00019-78-C-0505
In Conjunction with IR&D Support

for

Department of the Navy
Naval Air Systems Command
Washington, D.C. 20361

by

James R. Kennedy
Research Department
Grumman Aerospace Corporation
Bethpage, N.Y. 11714

Approved for Public Release; Distribution Unlimited

Grumman Research Department Report RE-630

FATIGUE BEHAVIOR OF SOLUTION TREATED AND QUENCHED Ti-6Al-4V

by

James R. Kennedy

Final Report on Contract N00019-78-C-0505
in Conjunction with IR&D Support

for

Department of the Navy
Naval Air Systems Command
Washington, D.C. 20361

May 1981

Approved by:

Richard A. Scheuing
Director of Research

UNCLASSIFIED

SECURITY CLASSIFICATION OF THIS PAGE *(When Data Entered)*

REPORT DOCUMENTATION PAGE	READ INSTRUCTIONS BEFORE COMPLETING FORM
1. REPORT NUMBER / 2. GOVT ACCESSION NO.	3. RECIPIENT'S CATALOG NUMBER
4. TITLE *(and Subtitle)* Fatigue Behavior of Solution Treated and Quenched Ti-6Al-4V	5. TYPE OF REPORT & PERIOD COVERED Final Report 6. PERFORMING ORG. REPORT NUMBER RE-630
7. AUTHOR(s) J. Kennedy	8. CONTRACT OR GRANT NUMBER(s) N00019-78-C-0505
9. PERFORMING ORGANIZATION NAME AND ADDRESS Research Department Grumman Aerospace Corporation Bethpage, New York 11714	10. PROGRAM ELEMENT, PROJECT, TASK AREA & WORK UNIT NUMBERS
11. CONTROLLING OFFICE NAME AND ADDRESS	12. REPORT DATE May 1981 13. NUMBER OF PAGES
14. MONITORING AGENCY NAME & ADDRESS*(if different from Controlling Office)*	15. SECURITY CLASS. *(of this report)* UNCLASSIFIED 15a. DECLASSIFICATION/DOWNGRADING SCHEDULE

16. DISTRIBUTION STATEMENT *(of this Report)*

Approved for public release; distribution unlimited

17. DISTRIBUTION STATEMENT *(of the abstract entered in Block 20, if different from Report)*

18. SUPPLEMENTARY NOTES

19. KEY WORDS *(Continue on reverse side if necessary and identify by block number)*

Fatigue, Ti-6Al-4V, Early Stage Fatigue Damage

20. ABSTRACT *(Continue on reverse side if necessary and identify by block number)*

The effect of solution treating and quenching on titanium alloy Ti-6Al-4V was studied as a means to improve its fatigue resistance. Four separate heats of Ti-6Al-4V rod and one heat of sheet material were solution treated at temperatures ranging from 825 to 1040°C, and then water quenched. Screening tests were performed on the rod materials by fatigue testing at one level of constant strain amplitude (≈± 1%) to determine the relative fatigue resistance and the overall heat treat responsiveness of each heat. Subsequently, selection of one heat was made for more complete evaluation of low and high cycle

DD FORM 1 JAN 73 1473 EDITION OF 1 NOV 65 IS OBSOLETE
S/N 0102-014-6601

UNCLASSIFIED

SECURITY CLASSIFICATION OF THIS PAGE *(When Data Entered)*

fatigue behavior and tensile properties. A relative measure of fatigue crack initiation resistance for various solution treated and quenched conditions of the sheet material was determined by acoustic emission.

The fatigue test results for these materials showed that solution treating at particular temperatures in the α - β field followed by quenching produced improvements in fatigue resistance compared to the annealed and solution treated plus aged conditions. The optimum solution treating temperature varied for each material, but typically was about 875 to 900°C. Strain-life data shows that for both low and high cycle fatigue, improvements in the fatigue characteristics of solution treated and quenched material ranged from 10 to 50% compared to the annealed condition.

Based on acoustic emission tests during fatigue cycling, solution treated and quenched material had improved resistance to early stage fatigue crack initiation. The optimum solution treated and quenched materials were characterized by low yield strength, low elastic moduli, high uniform and total strains, and high work hardening rates. During cyclic loading these materials also exhibited significantly lower rates of strain softening indicating higher cyclic stability than annealed or aged material. Based on these results and previous work, the improved fatigue resistance appears to be related to strain induced transformation of retained β phase, which results in cyclic energy dissipation instead of rapid fatigue damage accumulation. The effects of solution treating and quenching appear to be general, thus suggesting the possibility of improved fatigue resistance in this class of titanium alloys.

CONTENTS

ILLUSTRATIONS

ILLUSTRATIONS (Cont)

ILLUSTRATIONS (Cont)

TABLES

ACKNOWLEDGMENTS

The author wishes to thank M. Valentine of Naval Air Systems Command for his interest as technical monitor for this program. I also wish to acknowledge J. Drauch, C. Horak, A. Hencken, W. Poit, P. Power, and R. Winter for technical assistance, and P. Adler, J. Papazian and A. Tobin for helpful technical discussions. Finally, acknowledgment to C. Gilmore and M. Imam of George Washington University for helpful technical discussions.

1 - INTRODUCTION

In designing high performance aircraft, we are concerned with the selection of structural materials that possess high reliability in the presence of complex loading spectrums. In particular, high fatigue crack initiation resistance and slow stable crack growth are material properties necessary for long operating life with high levels of safety and durability. The majority of critical structural components on aircraft are fatigue limited, and in many cases, the time for fatigue crack initiation may represent 80-90 percent of total part life. Also, there are various components (e.g., wing pivots) classified as "single load-path take-out points" whose service lives are directly dependent on fatigue crack initiation. Since structures are designed to meet fatigue requirements under various notched and spectrum loading conditions, a material offering increased total fatigue life is considered of great importance. Fatigue life improvements of only two times or greater are significant to aircraft designers in terms of reliability and service life.

Recent work cited by Gilmore and Imam (Refs. 1 to 4) on the fatigue properties of annealed and martensitic Ti-6Al-4V (Ti 6/4) showed significant improvements in torsional fatigue life as a result of solution treating at 900°C and water quenching (STQ 900). The STQ 900 treatment had the longest fatigue life compared to other ST temperatures by at least a factor of four. A comparison with the alpha + beta ($\alpha + \beta$) annealed condition demonstrated that the STQ 900 condition resulted in an order of magnitude improvement of strain-life characteristics. These results are shown in Figures 1 and 2. Tensile strength and ductility for the STQ 900 condition were also higher relative to commonly used annealing treatments. In a limited investigation of axial fatigue properties, Gilmore and Imam (Ref. 5) also showed that the fatigue life of the STQ 900 material under constant load amplitude was about 35 times greater than for the ($\alpha + \beta$) annealed condition.

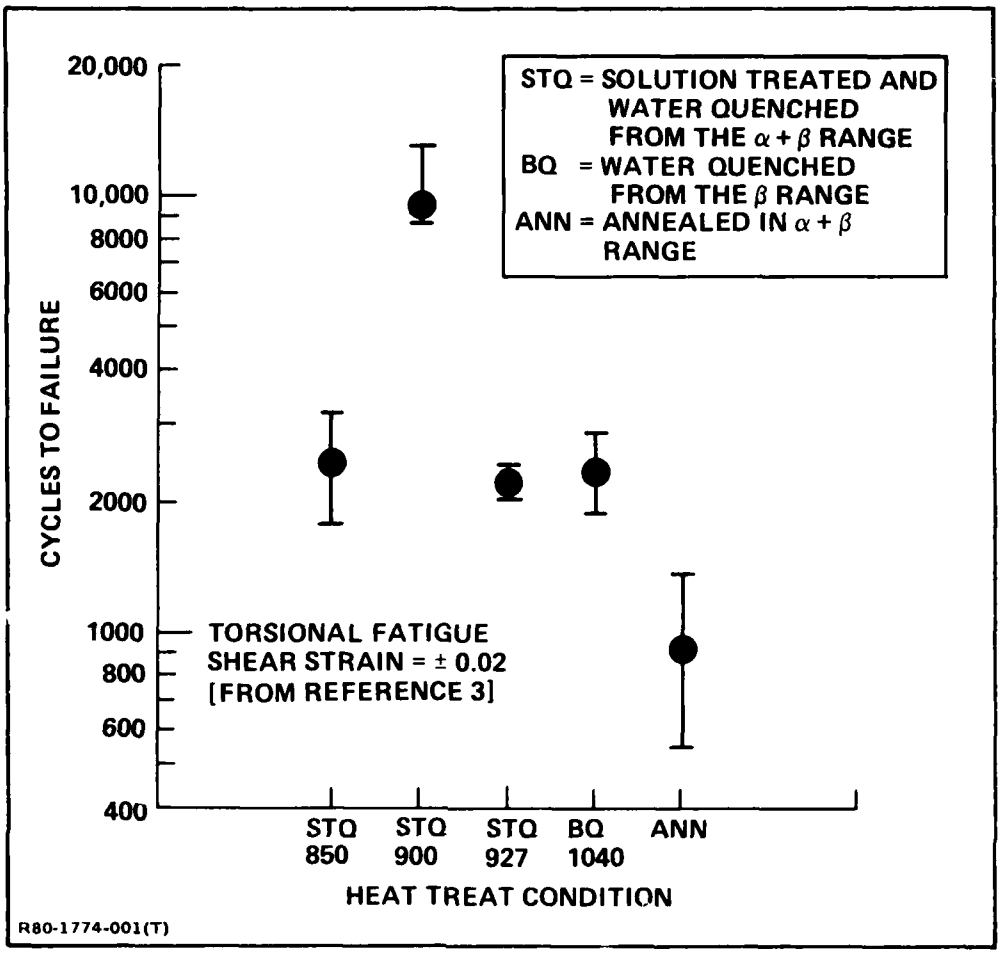

Figure 1. Comparison of torsional fatigue lifetimes in Ti-6Al-4V rod, 9.5 mm diameter (Code D).

Although the reasons for increased fatigue life in the STQ 900 condition are not completely understood, Gilmore and Iman (Ref. 3) believe that it is due to either a strain-induced martensite transformation effect or to the presence of a very finely dispersed martensitic structure. Their most recent microstructural observations indicated that strain accommodation by a strain-induced transformation of retained β to martensite occurs rather than localized plastic deformation that produces fatigue damage. It is recognized in titanium that the β phase, produced with just sufficient stabilizing content to be retained by quenching, will form martensite as a result of straining (Refs. 6 to 8). These results are of interest because of their potential in the future design of more fatigue

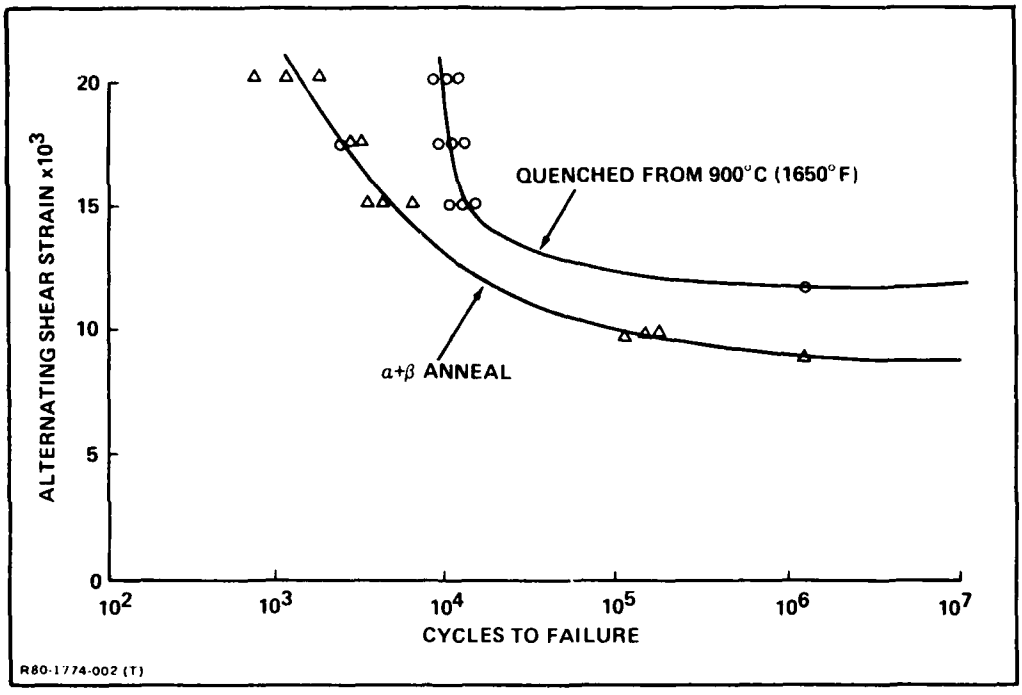

Figure 2. Cycles to failure as a function of the applied alternating shear strain for Ti-6Al-4V specimens $\alpha + \beta$ annealed and solution-treated at 900°C and water quenched (taken from Ref. 3)

resistant and reliable structural components. A material offering significantly improved fatigue crack initiation resistance and a longer fatigue life could lead to the design of more efficient structural components.

The improved fatigue lifetimes of the STQ 900 condition reported by Gilmore were mainly demonstrated by torsional fatigue testing of a single heat of the fine grained, small diameter Ti 6/4 bar stock. To more fully assess the potential of solution treating and quenching as a means of significantly improving fatigue life of Ti 6/4 for engineering applications it was considered essential to determine the axial fatigue behavior of this heat treat condition for various heats of the alloy. Variables such as solution treating temperature, microstructural characteristics, and strain amplitude were considered.

2 - EXPERIMENTAL PROCEDURES

2.1 GENERAL APPROACH

A screening test evaluation was conducted on four separate heats of Ti 6/4 rod and one heat of sheet material to determine their response to heat treat modification, and to determine optimum solution treating temperatures for each heat. The screening tests enabled the comparison of several conditions for each heat, mainly consisting of:

- 4 STQ
- 1 Annealed (ANN)
- 1 Solution treated and aged (STA)
- Beta field quench (BQ).

The screening evaluation was based on conducting axial fatigue tests on each condition at one level of cyclic loading, representing the low cycle fatigue region. A comparison of fatigue lifetimes was made to determine a) relative fatigue resistance of each condition, and b) overall heat treat responsiveness of each candidate heat. Based on these test results, selections were made for more complete evaluation, including static tensile and high and low cycle fatigue testing. In addition, a relative measure of fatigue crack initiation resistance for various solution treated and quenched conditions of the Ti 6/4 sheet material was determined utilizing an acoustic emission technique.

2.2 SPECIMEN PREPARATION

The starting material was mill-annealed Ti 6/4 and consisted of the following:

1) Round Bar

- 19 mm diameter (CODE A)
- 25.4 mm diameter (CODE B)

- 9.5 mm diameter (CODE D)
- 6.4 mm diameter (CODE K)

2) Sheet

- 3.2 mm thick (CODE P).

The chemical composition for each material is shown in Table 1. The analysis of the original material upon which Gilmore and Imam conducted their experiments (6.4 mm diameter rod) is also included in Table 1 for comparison.

TABLE 1. CHEMICAL ANALYSES OF Ti-6Al-4V MATERIAL.

MATERIAL DESCRIPTION	CHEMICAL COMPOSITION						
	WEIGHT %				PPM (WEIGHT %)		
SIZE, CODE	Al	V	Fe	C	O	H	N
12.7 mm, A	6.6	4.4	0.2	0.03	1630	52	140
12.7 mm, B	6.8	4.2	0.08	0.02	1535	49	160
9.5 mm, D	6.5	3.9	0.2	0.03	1385	48	120
6.4 mm, K	6.3	4.0	0.2	.03	1700	83	200
3.2 mm, P	6.3	3.6	0.13	.03	1770	43	120
6.4 mm, G*	5.8	3.7	0.2	.04	1390	74	140

*Code G represents Grumman analysis of original 6.4 mm diameter rod obtained from Gilmore and Imam.

R80-1774-032(T)

The 19 mm and 25.4 mm diameter rods were reduced to 12.7 mm in diameter prior to heat treating. The other materials were heat treated at their original sizes. All rods were heat treated in lengths of 152.4 mm; the sheet material was heat treated in strips 15.88 mm wide x 228.6 mm long. The heat treating procedures used for the 12.7 mm and 9.5 mm diameter rods (i.e., Codes A, B, and D) are shown in Table 2.

TABLE 2. HEAT TREAT SCHEDULES.

HEAT TREAT DESIGNATION	HEAT TREAT PROCEDURE
1) STQ 850	850°C/1 hr → Water Quench (WQ)
2) STQ 875	875°C/1 hr → WQ
3) STQ 900	900°C/1 hr → WQ
4) STQ 925	925°C/1 hr → WQ
5) ANN	800°C/1 hr → Furnace cool to 500°C then air cool
6) STA	900°C/1 hr → WQ + 540°C/4 hours, air cool
7) BQ 1040	1040°C/1 hr → WQ
R80-1774-033(T)	

All specimens were heat treated in air. Quenching was accomplished by removing the specimens individually from the furnace and plunging them vertically (end first) into a cold water bath. The time between removal of a specimen from the furnace and quenching was two seconds or less. After heat treating, the specimens were checked for quench distortion by rolling them over a flat ground plate; specimens which exhibited some form of distortion, such as bending, were eliminated from further testing.

The subsequent heat treating of the 6.4 mm diameter rods (Code K) and the 3.2 mm sheet (Code P) was basically the same as the other materials, with the following exceptions: the beta field quench was eliminated from further evaluation based on the test results of the other materials, and the solution treating hold time was reduced to 10 min. because of the smaller section sizes.

After heat treating, the microstructures of representative test pieces were checked for microstructural uniformity for each of the various heat treatments. The microstructures of each group of specimens were found to be essentially uniform. The oxide layers formed on each rod specimen as a result of heat treatment were completely removed during subsequent machining operations. The oxide layers on the sheet specimens were removed by chemical milling. All specimens were inspected by optical microscopy and hardness testing to insure that any oxygen diffusion zone was completely removed.

Fatigue test specimens were then machined from the heat treated material. The fatigue specimen configurations are shown in Figures 3a and 3b. The surface of each specimen was hand finished by polishing with No. 600 SiC abrasive paper.

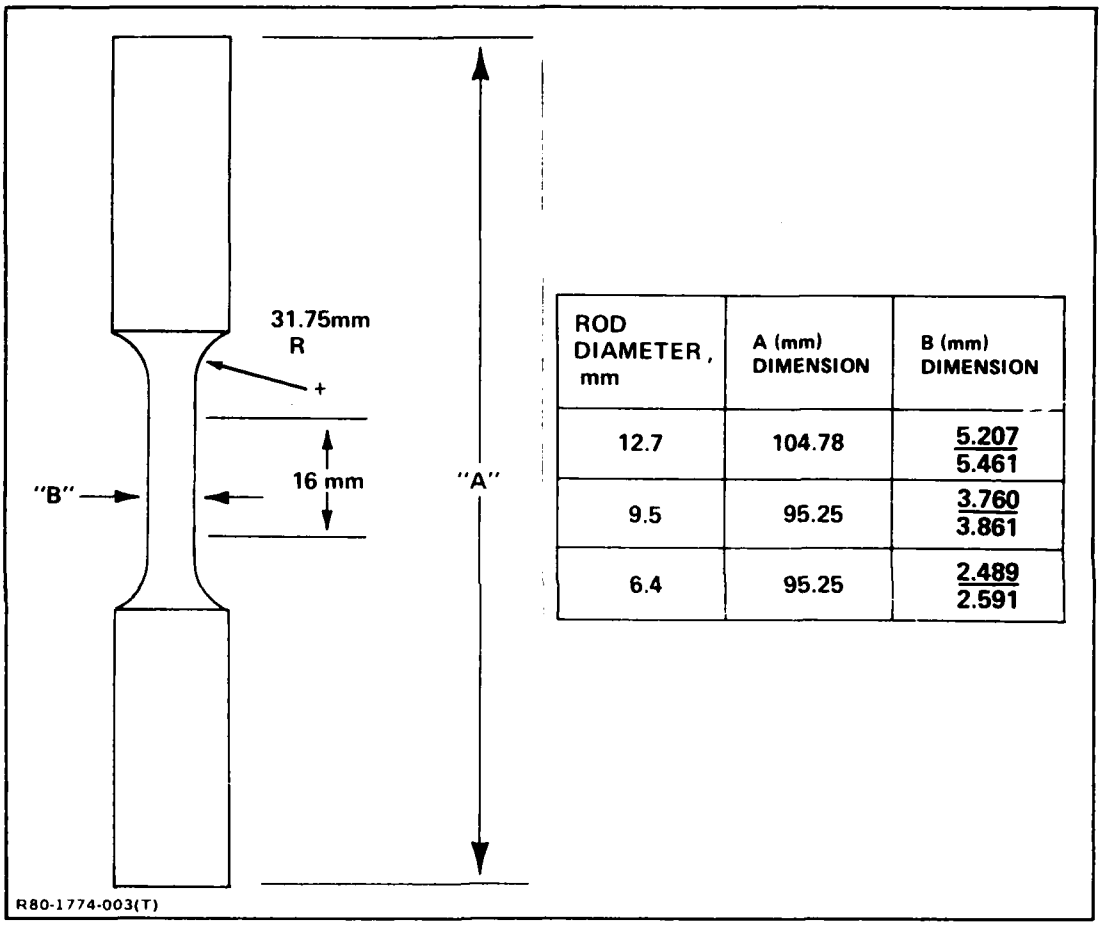

ROD DIAMETER, mm	A (mm) DIMENSION	B (mm) DIMENSION
12.7	104.78	5.207 / 5.461
9.5	95.25	3.760 / 3.861
6.4	95.25	2.489 / 2.591

Figure 3a. Round axial fatigue and tensile specimen configuration.

2.3 FATIGUE AND TENSILE TESTING

Fatigue and tensile testing were performed in accordance with current standards of good practice. All rod specimens were tested in fatigue, using constant amplitude strain controlled tests with zero mean strain. Self-aligning Wood's metal grips were used to reduce residual bending strains due to misalignment. Fatigue of the specimens was performed on an MTS servo-hydraulic

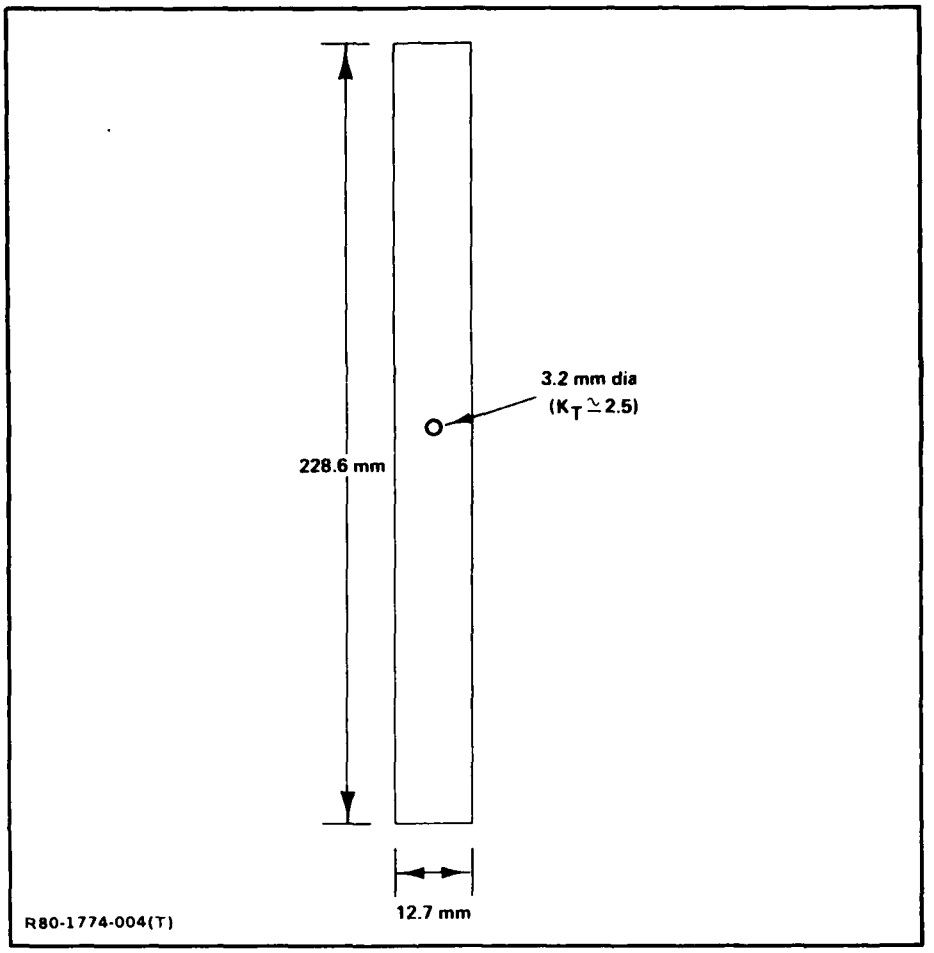

Figure 3b. Center-notched sheet fatigue specimen.

testing machine, with a clip-on extensometer providing the signal for strain control of the low cycle tests. The extensometer was used in all low cycle fatigue tests where straining exceeded the elastic limit of the material. The extensometer was not used in high cycle fatigue tests that were conducted below the elastic limit of the specimen; in these tests, the specimens were fatigued using constant amplitude load control, at loads corresponding to the selected test strains.

The screening evaluation for the rod specimens was performed at strain amplitudes of 0.9 to 1.1 percent, depending on the rod diameter. In this phase, one specimen per heat treat condition was tested. Based on the screening

evaluation, additional tests were conducted on selected materials at strain amplitudes ranging from 0.5 to 1.1 percent strain. During strain controlled testing, both strain and load levels were recorded to provide information on the cyclic deformation behavior of each heat treat condition. All fatigue tests on the sheet material were conducted using constant amplitude load control at a stress ratio of R = 0.05 (R = minimum load/maximum load). Tensile tests were conducted in accordance with current conventional practice; specimens were loaded at a constant strain rate of 1%/minute.

2.4 ACOUSTIC EMISSION TESTS

A relative measure of fatigue crack initiation resistance for various solution treated conditions of the Ti 6/4 sheet was determined by an acoustic emission technique. Sheet specimens were used because of the ease in attaching acoustic emission sensors to flat surfaces.

The application of acoustic emission to study fatigue crack initiation is being developed as part of an in-house effort. The Grumman-designed acoustic system is capable of detecting acoustic emission event signals in a background of extraneous noise signals at all levels. The system is based on a threshold-crossing counting technique, which determines the number of events that exceed a certain threshold voltage value. The system utilizes wave form conditioning, spatial discrimination, and wave form discrimination to identify and reject extraneous noise signal data from computer processing. A combination of "master-slave" piezoelectric type sensors with maximum sensitivity at a resonant frequency of 280-320 kHz were utilized; the nominal threshold detection level was 0.5 volt.

2.5 MICROSTRUCTURAL AND FRACTOGRAPHIC CHARACTERIZATION

Optical metallography specimens were prepared by standard polishing techniques. Specimens were polished to a 0.05 μm alumina finish and etched with Krolls reagent. Fracture surfaces were examined using scanning electron microscopy. Hardness tests were conducted on various heat treat conditions using Knoop microhardness.

3 - RESULTS

3.1 MICROSTRUCTURES

Representative microstructural changes produced for each Ti-6Al-4V alloy as a result of heat treating according to the schedules listed in Table 2 are shown in Figures 4 to 8. As expected, there is a general similarity between the microstructures of each corresponding heat treat condition. In each case, the α-β annealed condition (ANN) consists of a matrix of primary α and particles of β in the grain boundaries. The materials which were solution treated and quenched from the β field (BQ) have a uniform distribution of α' martensite resulting from the transformation of prior massive β grains. The microstructures produced by solution treating and quenching from the α-β field (STQ) consist of mixtures of primary α and a quenched transformation product, which appears to consist mainly of α' martensite. It is widely accepted that hexagonal martensite, α' is usually formed upon quenching, although other forms, such as orthorhombic, are also possible. X-ray diffraction measurements were made of the STQ conditions to determine if β phase was present but only the α phase was observed. A more detailed phase analysis of the quenched transformation product was not conducted as part of this work. The solution treated and aged (STA) conditions mainly consist of mixtures of primary α and the tempered martensite structure of Widmanstatten $\alpha + \beta$.

For these alloys, the volume fraction of primary α in the STQ condition ranged from approximately 80 percent at the lowest solution treating temperature (STQ 850) to 40 percent at the highest temperature (STQ 925). In each alloy, even though the volume fraction of primary α decreased with increasing solution treating temperature, the size of the primary α grains remained basically consistent for all STQ conditions. For the 12.7 mm dia rods (CODE A and B) the primary α size in the STQ conditions was approximately 5 μm, and for the other materials the size was about 3 μm. Micrographs of the STQ conditions which exhibited the highest fatigue life within each heat of material are

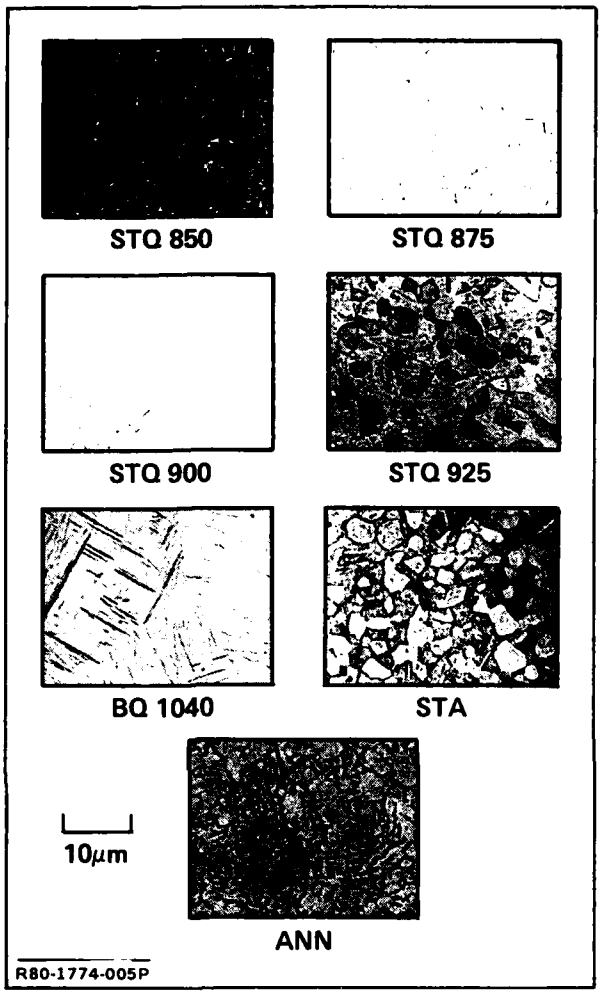

Figure 4. Microstructures of heat treated 12.7 mm diameter Ti-6Al-4V rod (Code A).

shown in Figures 9 to 11. In each case, a fine α' Widmanstatten structure exists within the transformed regions of the microstructure. In these STQ conditions, the α' martensite platelet spacings were ≤ 0.5 μm; a list of α' platelet spacings, sizes, and α volume fractions is shown in Table 3. Volume fractions were determined by grid point counting. This fine α' structure was also characteristic of the other STQ conditions.

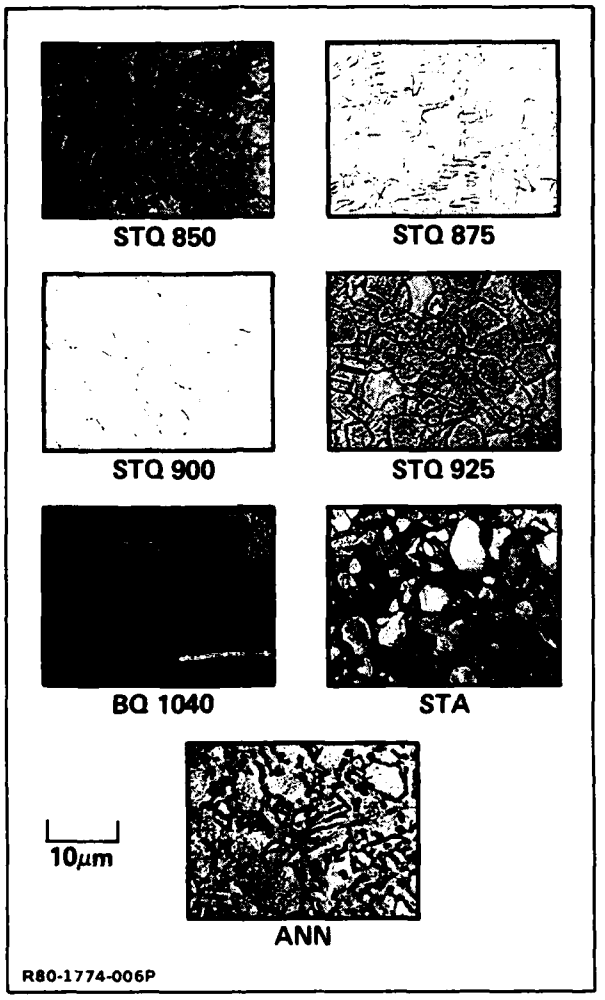

Figure 5. Microstructures of heat treated 12.7 mm diameter Ti-6Al-4V rod (Code B).

3.2 FATIGUE RESULTS

The initial fatigue evaluation of the solution treated and quenched condition was conducted at relatively high strain amplitudes primarily because the previous work reported by Gilmore and Imam (Ref. 2) demonstrated that fatigue life improvements due to the STQ conditions were readily observed at high strains. In the present work, in order to avoid compressive buckling, the 12.7 mm and 9.5 mm diameter rods were tested at a maximum strain of ± 0.011; the 6.4 mm diameter rod was limited to ± 0.009 maximum strain.

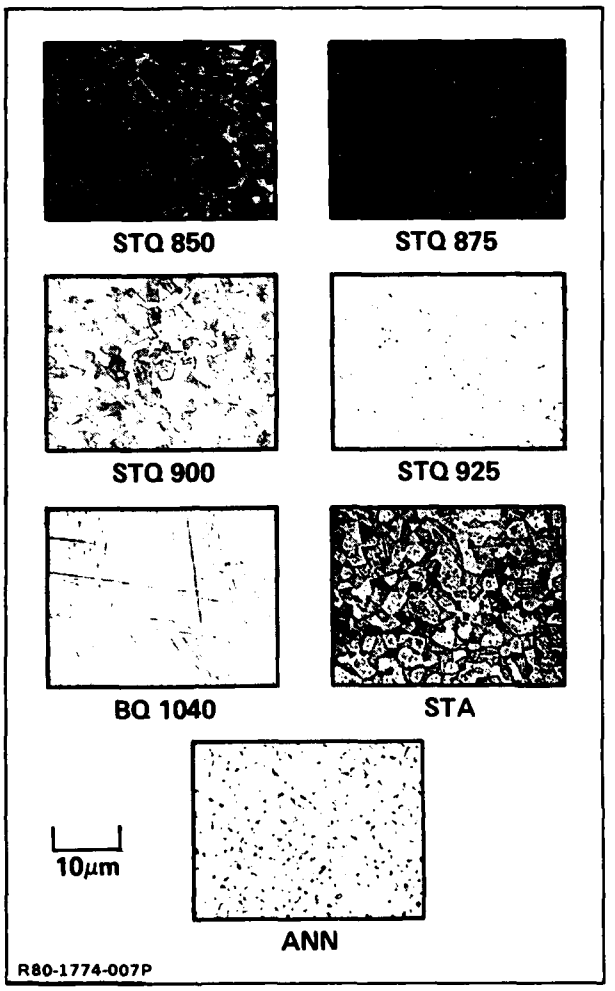

Figure 6. Microstructures of heat treated 9.5 mm diameter Ti-6Al-4V rod (Code D).

The results of fatigue testing at constant strain amplitude in the low cycle fatigue life range for the rod materials is shown graphically in Figures 12 to 15, which present comparisons of fatigue lifetimes for each heat treat condition. The complete fatigue lifetime data for all the rod material is presented in Tables 4 to 6. It can be seen that for each heat of Ti-6Al-4V there was an apparent optimum solution treating (ST) temperature at which at least one STQ condition had a longer fatigue life than all of the other conditions. Replication fatigue tests were conducted on a few selected heat treat conditions as indicated in the data.

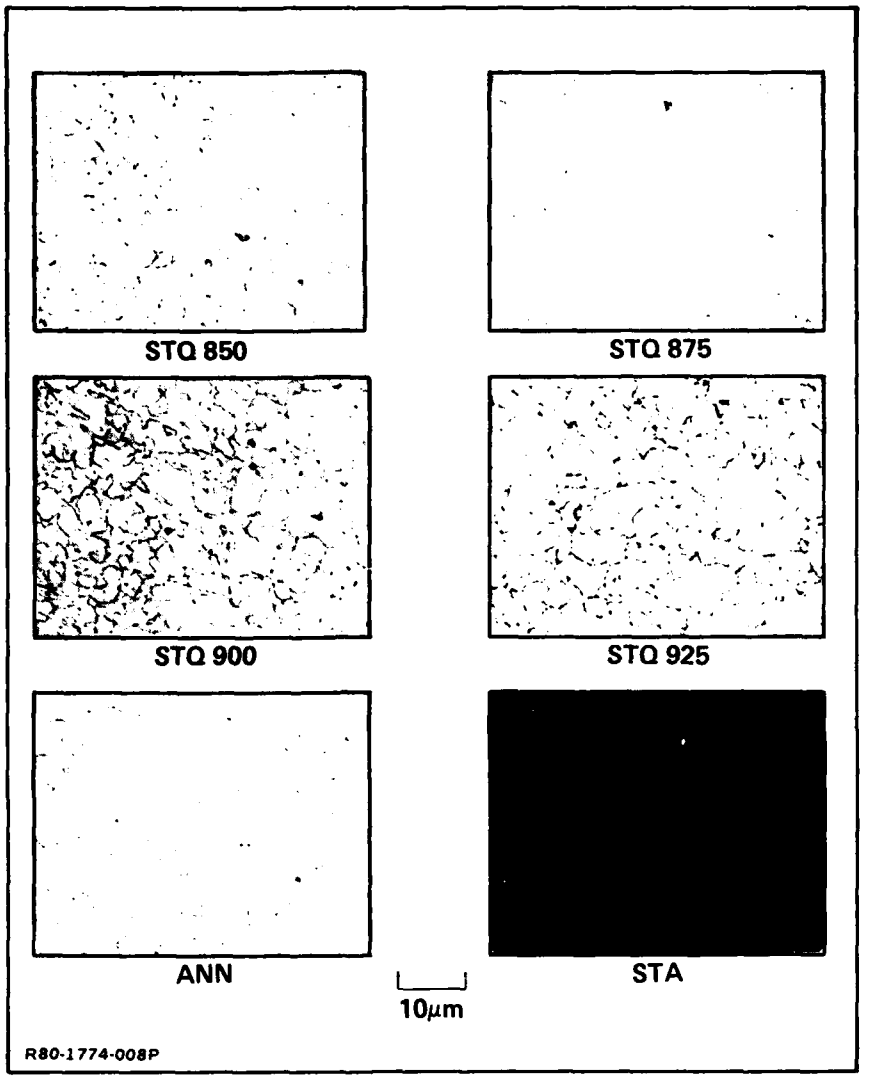

Figure 7. Microstructures of heat treated 6.4 mm diameter Ti-6Al-4V rod (Code K).

It is significant that each heat of Ti-6Al-4V responds to solution treating and quenching in a similar manner. For each heat there appears to be a critical ST temperature (or temperature range) associated with improved fatigue resistance. The ST temperatures associated with maximum fatigue life for each heat is as follows:

- 12.7 mm rod (CODE A) - 900-925°C
- 12.7 mm rod (CODE B) - 900-925°C

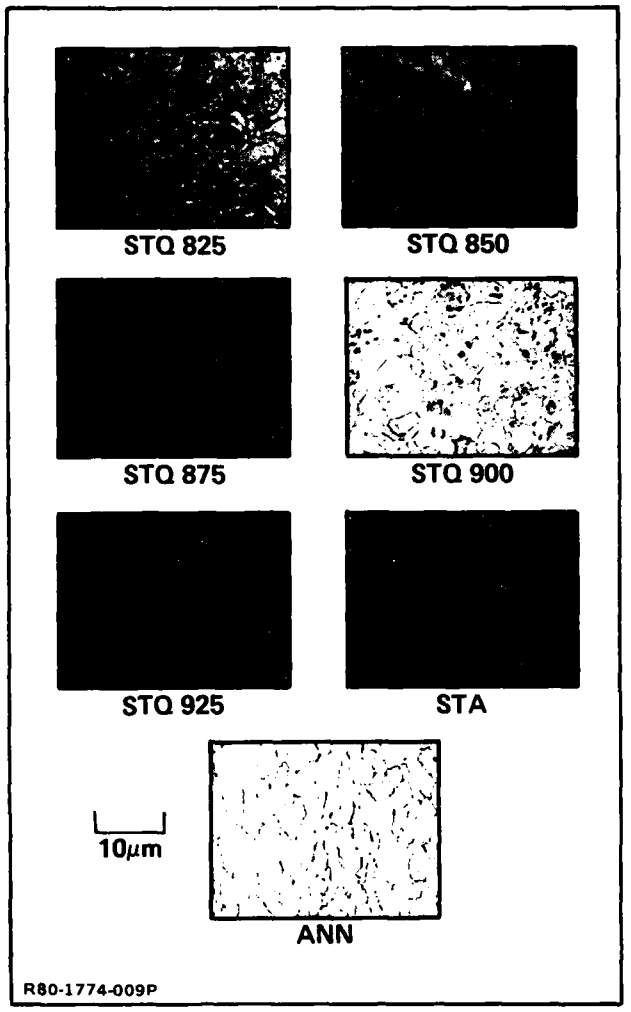

Figure 8. Microstructures of heat treated 3.2 mm thick Ti-6Al-4V sheet (Code P).

- 9.7 mm rod (CODE D) - 850-875°C
- 6.4 mm rod (CODE K) - 900°C.

These data, which represent axial loading, are in general agreement with Figure 1, which represents torsional loading.

The extent and variation of fatigue life improvement of the STQ condition for each heat is made by comparing the ratio of lifetimes of the annealed and STA conditions, which is shown in Table 7. Compared to the annealed condition, the fatigue life of the STQ condition is approximately 1.2 to 2.7 times better in

Figure 9. Solution treated and quenched microstructures: top – 12.7 mm rod, Code A, STQ 900; bottom – 12.7 mm rod, Code B, STQ 900.

these materials, and 1.2 to 1.9 times better than the STA condition. From the torsional fatigue data in Figure 1 the STQ 900 condition is 10 times better than the annealed condition. In other unpublished work conducted by Imam (Ref. 10) on the same 6.4 mm diameter rod (CODE K) used in this work, it was found that the STQ 900 condition had a torsional fatigue life (strain = ±0.02) about six times longer than the annealed condition. It should be emphasized that the data based on torsional fatigue are not considered to be directly comparable to the axial data because of basic differences in the loading modes.

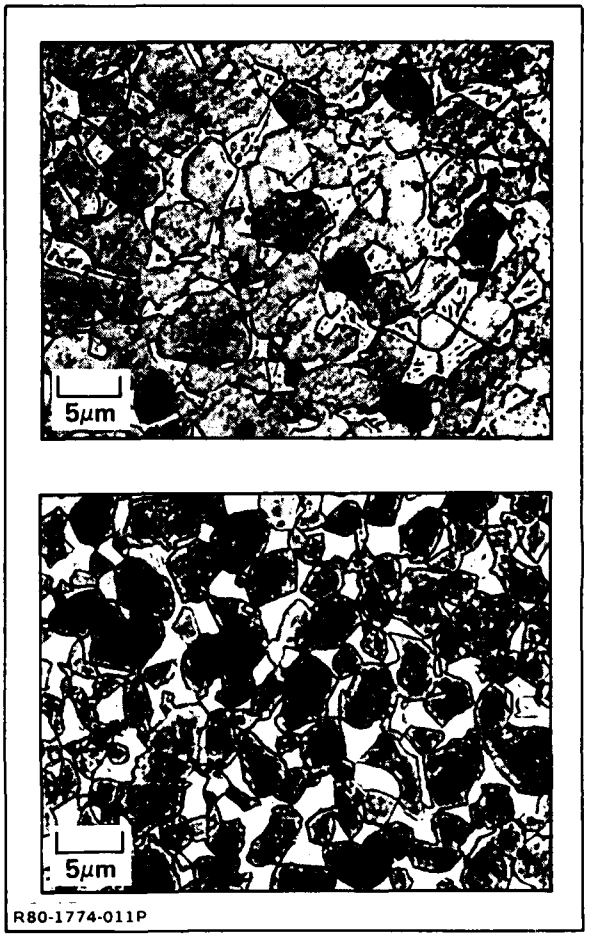

Figure 10. Solution treated and quenched microstructures: top – 9.5 mm rod, Code D, STQ 875; bottom – 6.4 mm rod, Code K, STQ 900.

The apparent fatigue resistance of the material evaluated in this work also varies. Maximum fatigue lifetimes (strain = ±0.011) of the CODE A, B, and D rods in the STQ condition are 2010, 1850, and 3550 cycles, respectively. At a strain of ±0.009, the fatigue lifetimes of the CODE D and K rods in the STQ condition are 7237 and 6767 cycles, respectively. The generally higher fatigue life of the 9.5 mm rod (CODE D) is attributed to its finer and more uniform microstructure of primary α ($\simeq 3$ μm) compared to the two 12.7 mm rods (CODES A and B) which have an average primary α grain size $\simeq 5$ μm. Although there are differences in the basic fatigue resistance of these materials, they have each

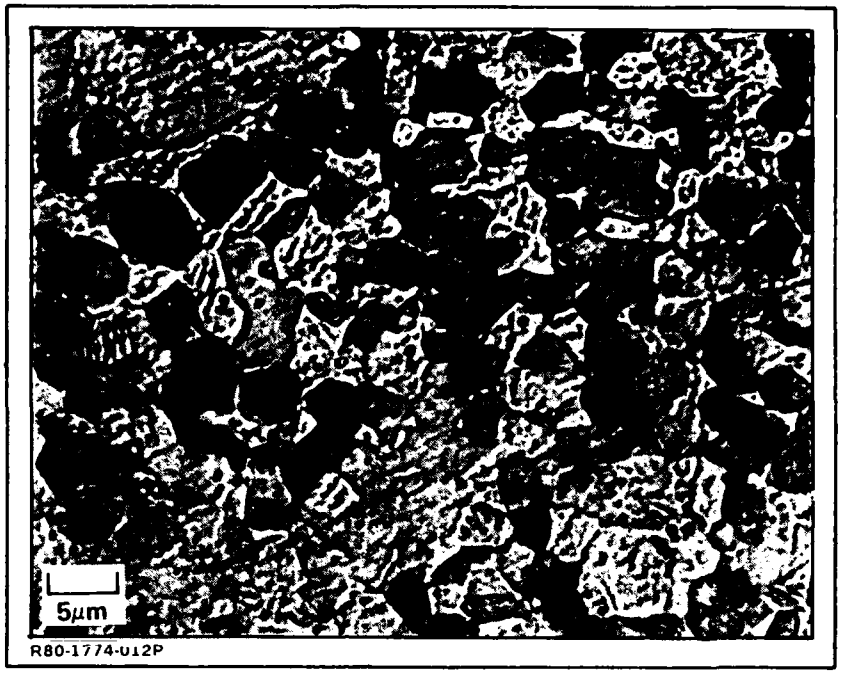

Figure 11. Solution treated and quenched microstructures of 3.2 mm sheet, Code P, STQ 875.

demonstrated some degree of improvement as a result of solution treating and quenching. In these relatively fine grained materials, the STQ conditions exhibiting the highest fatigue lifetimes are characterized by a mixture of primary α

TABLE 3. SUMMARY OF MICROSTRUCTURAL FEATURES OF VARIOUS HEAT TREAT CONDITIONS IN Ti-6Al-4V.

MATERIAL CONDITION	PRIMARY ALPHA GRAIN SIZE, μ m	VOLUME FRACTION OF PRIMARY ALPHA	SPACING OF α' PLATELETS IN TRANSFORMED BETA, μ m
A (12.7 mm) STQ 900	5.1	0.58	0.40
B (12.7 mm) STQ 900	5.2	0.57	0.46
D (9.5 mm) STQ 875	3.2	0.67	0.37
K (6.4 mm) STQ 900	3.0	0.73	0.41
P (3.2 mm) STQ 875	3.0	0.64	0.55
G* (6.4 mm) STQ 900	3.6*	0.57*	0.5*

(*Ref. 1, 4)

R80-1774-034(T)

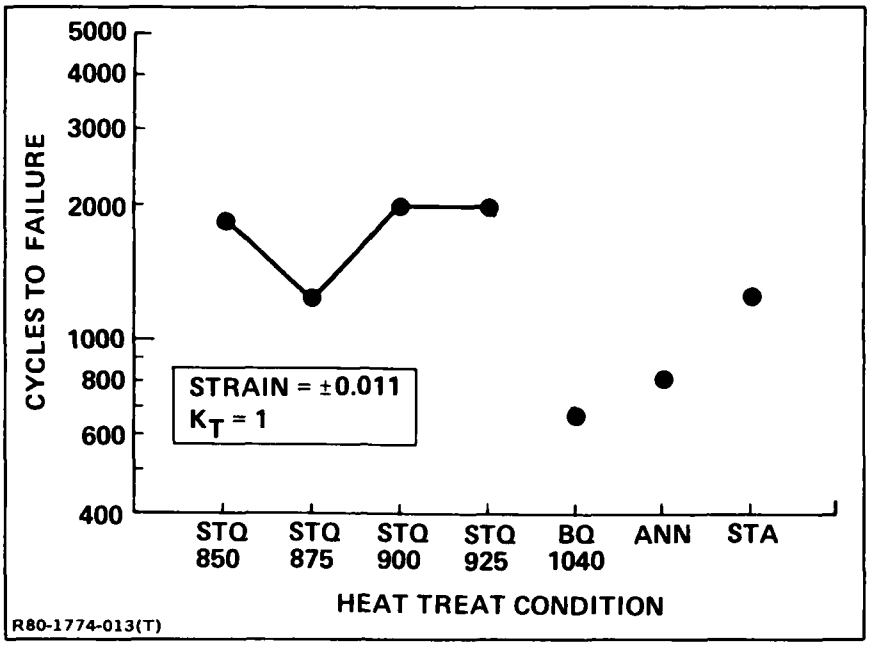

Figure 12. Comparison of fatigue lifetimes in Ti-6Al-4V (Code A) rod - 12.7 mm diameter.

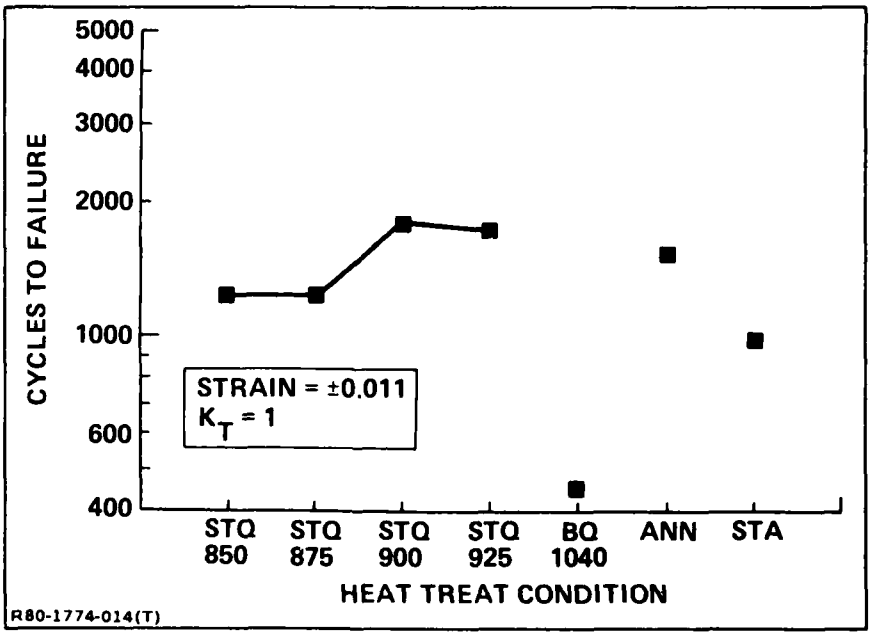

Figure 13. Comparison of fatigue lifetimes in Ti-6Al-4V (Code B) rod - 12.7 mm diameter.

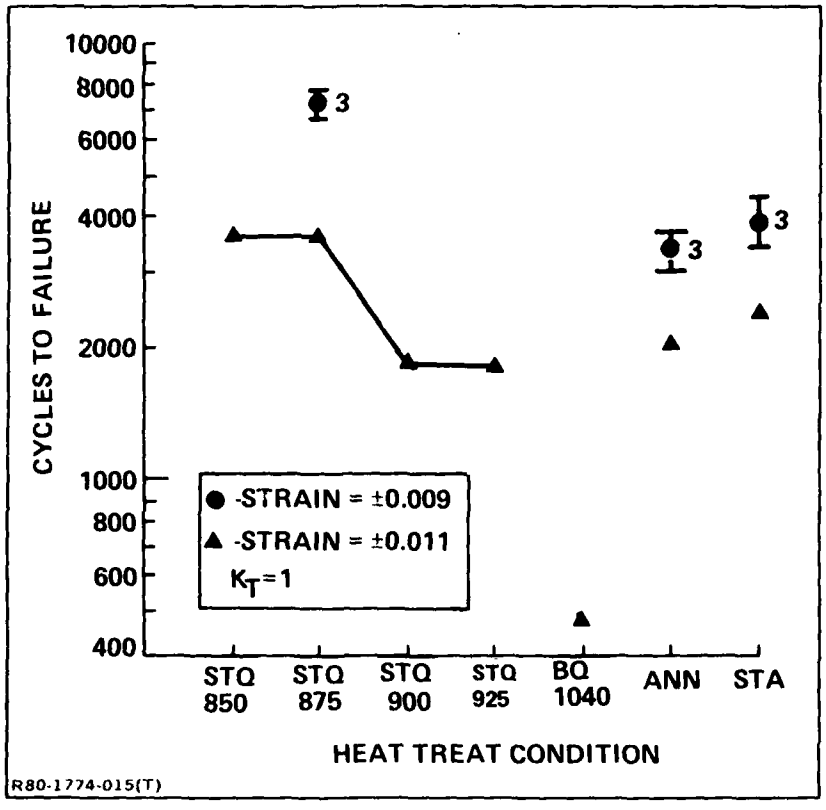

Figure 14. Comparison of fatigue lifetimes in Ti-6Al-4V (Code D) rod - 9.5 mm diameter.

(average volume fraction = 0.64±0.076) and a quenched transformation structure, largely consisting of finely spaced ($\leq$0.5 μm) martensite platelets. The actual presence and extent of retained beta in the quenched structure, which according to Gilmore and Imam was responsible for the fatigue life improvement in their material, is an important consideration, but remains to be determined for the materials in this work. It is of interest that the materials quenched from the 100 percent β range (BQ 1040), resulting in a 100 percent martensitic structure presumably with no retained β, exhibited the lowest fatigue lifetimes. In contrast, the BQ 1040 condition shown in Figure 1, tested in torsional fatigue, had a lifetime about 2-1/2 times longer than annealed condition of the same material. It is not clear if these differences between the axial and torsional data for the BQ 1040 condition are due to basic material characteristics or inherent differences in the loading mode of each test.

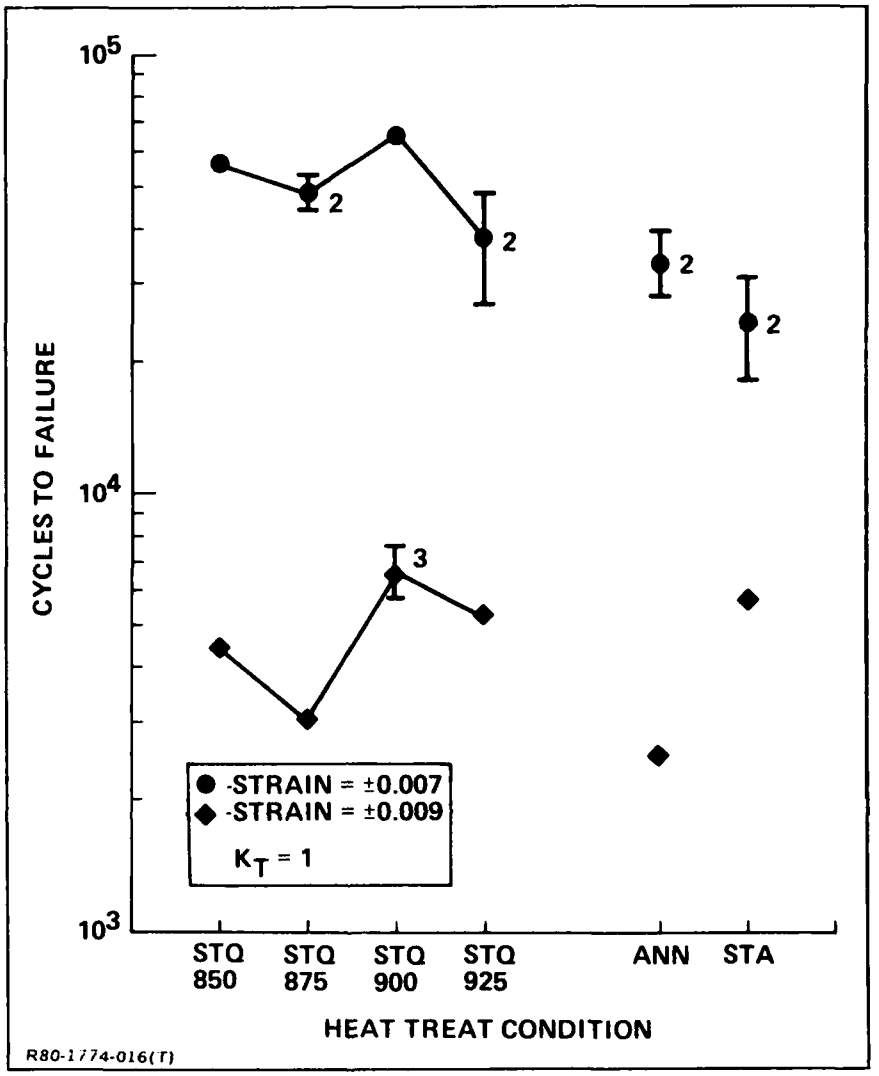

Figure 15. Comparison of fatigue lifetimes in Ti-6Al-4V (Code K) rod - 6.4 mm diameter.

On the basis of the low cycle fatigue results described above it was decided to eliminate the 12.7 mm rods from further testing and further characterize the 9.5 mm and 6.4 mm material. The 9.5 mm rod was selected for more extensive fatigue testing primarily because it appeared to be the most generally fatigue resistant than the others. The 6.4 mm rod was received after the start of this program but was of interest because Imam (Ref. 10) had conducted a small number of torsion fatigue tests on the same material and established that the STQ

TABLE 4. COMPARISON OF FATIGUE LIFETIMES IN HEAT TREATED Ti-6Al-4V ROD AT CONSTANT STRAIN CYCLING.

HEAT TREAT CONDITION	CYCLES TO FAILURE, N_f		
	12.7 mm - CODE A	12.7 mm - CODE B	9.5 mm - CODE D
STQ 850	1878	1250	3597
STQ 875	1254	1250	3550
STQ 900	2010	1852	1846
STQ 925	2000	1784	1793
BQ 1040	669	454	470
ANN	800	1549	2011
STA	1250	986	2372
(TOTAL STRAIN AMPLITUDE = ±0.011)			

R80-1774-035(T)

TABLE 5. SUMMARY OF FATIGUE LIFETIMES IN Ti-6Al-4V ROD-9.5mm (CODE D).

TOTAL STRAIN AMPLITUDE	HEAT TREAT CONDITION [N_f = CYCLES TO FAILURE]		
	STQ 875 N_f	ANN N_f	STA N_f
± 0.011	3550	2011	2372
± 0.009	7725 6985 7000	3695 3463 2996	3400 3630 4490
± 0.007	60,360 382,000	32,740	20,820
± 0.065	127,720 59,480 1.24×10^7 (DNF)	36,920 24,740 86,260	38,690 19,810 77,400
± 0.006	5.1×10^6 (DNF)	49,280	2.3×10^6 (DNF)
± 0.0055	–	3.9×10^6 (DNF)	2.6×10^6 (DNF)
DNF = DID NOT FAIL			

R80-1774-036(T)

TABLE 6. SUMMARY OF FATIGUE LIFETIMES FOR Ti-6Al-4V ROD - 6.4 mm (CODE K).

TOTAL STRAIN AMPLITUDE	HEAT TREAT CONDITION [N_f = CYCLES TO FAILURE]					
	STQ 850 N_f	STQ 875 N_f	STQ 900 N_f	STQ 925 N_f	ANN N_f	STA N_f
± 0.009	3056	4482	6600 7729 5973	5209	2500	5874
± 0.007	57170	44730 53290	66090	27050 48760	28180 39540	18190 31700 47360
± 0.0067	–	61360	90790	550,590	40510	1.5×10^6 (DNF)
DNF = DID NOT FAIL						

R80-1774-037(T)

900 condition had improved fatigue life compared to the annealed condition. It would have been desirable to include the original 6.4 mm rod used by Gilmore and Imam (Ref. 4) in this work, but that was not possible because their material had been completely expended.

TABLE 7. COMPARISON OF LIFETIME RATIOS BETWEEN HEAT TREAT CONDITIONS IN Ti-6Al-4V ROD.

Ti-6Al-4V MATERIAL	$\frac{N_f \text{ (STQ max)}}{N_f \text{ (ANN)}}$ @ϵ = ±0.011	$\frac{N_f \text{ (STQ max)}}{N_f \text{ (ANN)}}$ @ϵ = ±0.009	$\frac{N_f \text{ (STQ max)}}{N_f \text{ (STA)}}$ @ϵ = ±0.011	$\frac{N_f \text{ (STQ max)}}{N_f \text{ (STA)}}$ @ϵ = ±0.009
12.7 mm (CODE A)	2.5	–	1.6	–
12.7 mm (CODE B)	1.2	–	1.9	–
9.5 mm (CODE D)	1.8	2.1	1.5	1.9
6.4 mm (CODE K)	–	2.7	–	1.2
(N_f = CYCLES TO FAILURE)				

R80-1774-038(T)

The results of low and high cycle fatigue testing of the 9.5 mm rod in the STQ, ANN, and STA conditions at constant strain amplitudes is shown as strain-life data in Figures 16 to 18, respectively. A comparison of the strain-life curves of these materials is shown in Figure 19. At the strain levels evaluated in this work the results show the STQ 875 condition to be clearly superior in its fatigue resistance in both the low and high cycle regimes. As expected, the amount of scatter in the fatigue life of each condition at 0.9 percent strain is relatively small. At the lower strains, between 0.6 and 0.7 percent, there was a greater spread in the lifetime data for each condition, which is generally consistent with high cycle behavior. By comparing the strain-life curves of the ANN and STQ 875 condition in Figure 19, it can be seen that the strain level of the STQ 875 condition is always higher than the ANN condition at any given corresponding lifetime. The increase in strain resistance of the STQ 875 compared to the ANN condition also varies over the total life. For example, at 4000 cycles, the strain level of the STQ 875 condition is about 50 percent higher; in the midlife region ($\approx 10^5$ cycles) the STQ 875 strain is approximately 10 percent higher; at 10^6 cycles, it is about 13 percent higher. Thus, a minimum improvement of approximately 10 percent in the strain-life characteristics has resulted in this material as a result of the STQ 875 heat treatment. Since the increased strain capability of the STQ 875 condition occurs over the entire life range evaluated, it is suggestive that the causative effect is more than just a manifestation of a high or low cycle fatigue characteristic of the material. For example, a highly ductile material would offer maximum cyclic strain resistance in the low cycle region, while a stronger material would be superior at high cyclic life. In comparison, the STQ 875 material can be characterized by good overall cycle strain resistance.

Fracture surfaces of the STQ 875, ANN, and STA conditions of the 9.5 mm rod were examined after testing at various strain levels. In all cases, fatigue crack initiation appeared to start at the specimen surfaces. The fracture surface topography was generally very similar between the specimens examined. Fatigue crack propagation near the initiation site seemed to occur by mixed

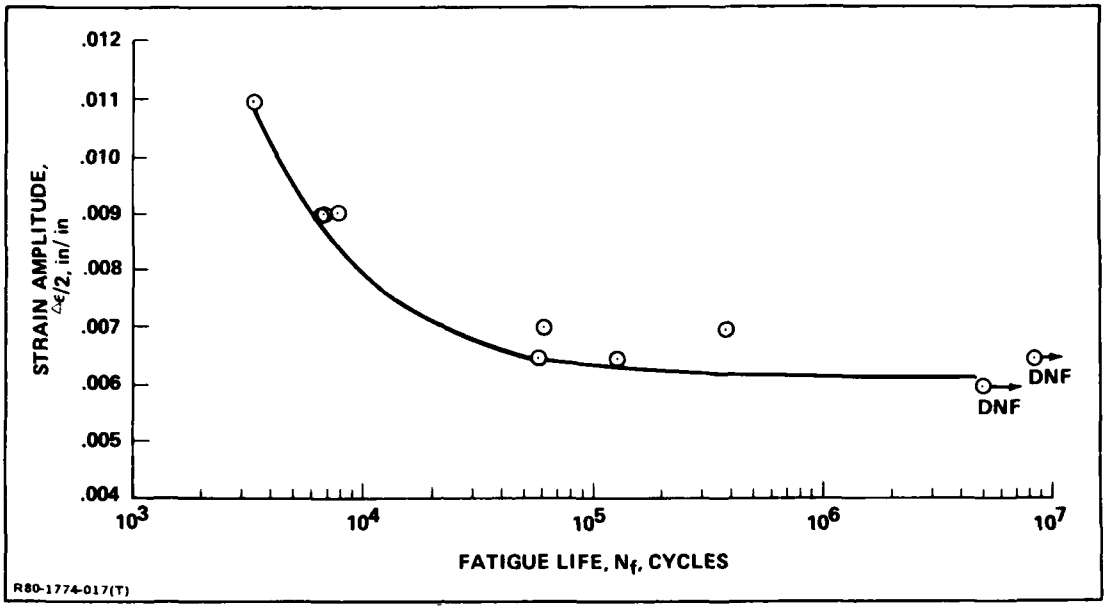

Figure 16. Strain-life curve of STQ 875 heat treat condition in Ti-6Al-4V rod – 9.5 mm diameter (Code D).

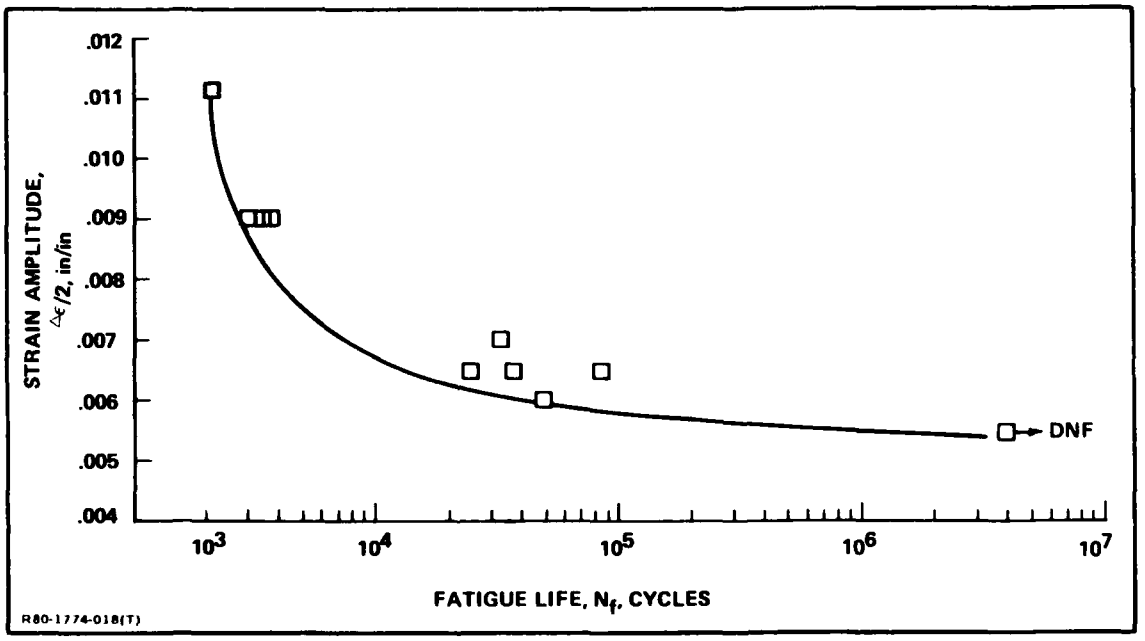

Figure 17. Strain-life curve of ANN heat treat condition in Ti-6Al-4V rod - 9.5 mm diameter (Code D).

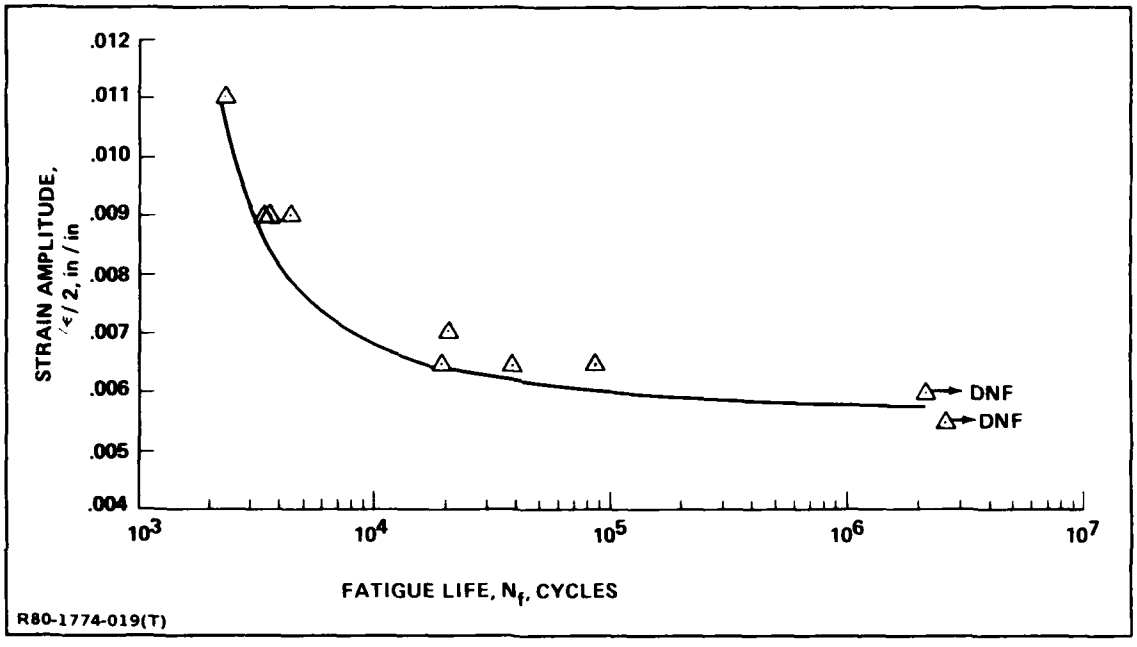

Figure 18. *Strain-life curve of* STA heat treat condition in Ti-6Al-4V rod – 9.5 mm diameter (Code D).

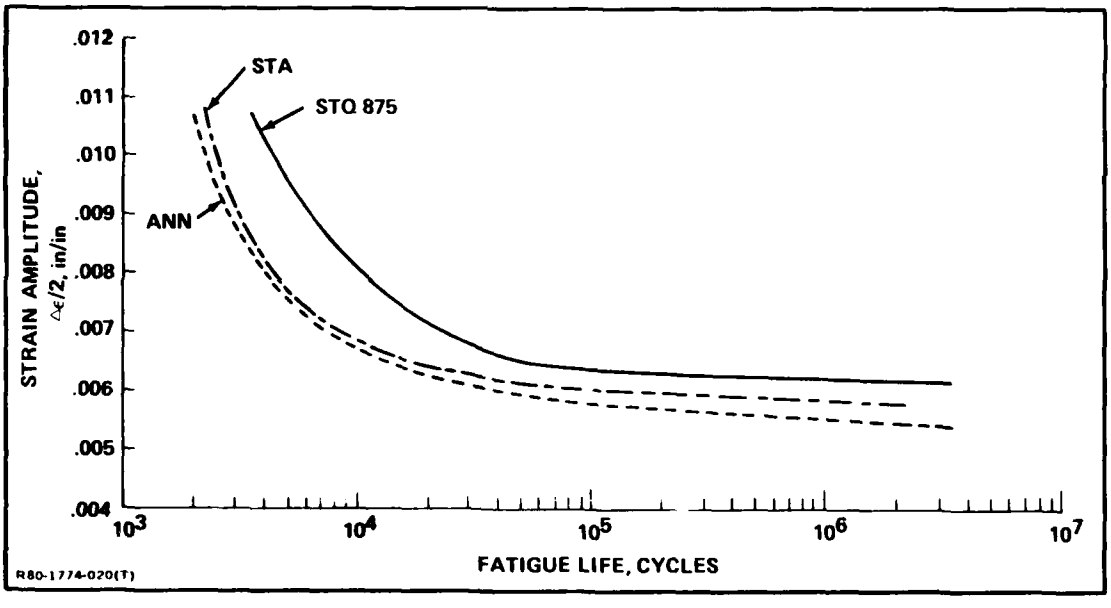

Figure 19. *Comparison of strain-life curves in* heat treated Ti-6Al-4V rod – 9.5 mm diameter (Code D).

modes consisting of "quasi"-cleavage of the primary α grains, quasi-cleavage at α/(α + β) interfaces, and striation formation. A comparison of fracture surfaces near the initiation site, after testing at 0.7 percent strain, is shown for these three conditions in Figure 20. The transgranular facets in each of these conditions correspond to the primary α particles. With continuing crack propagation into the specimens, the mixed mode persisted but with more evidence of secondary cracking, apparently at α/(α + β) interfaces. At higher crack growth rates, striation formation of primary α particles and ductile tearing of regions containing beta was commonly observed.

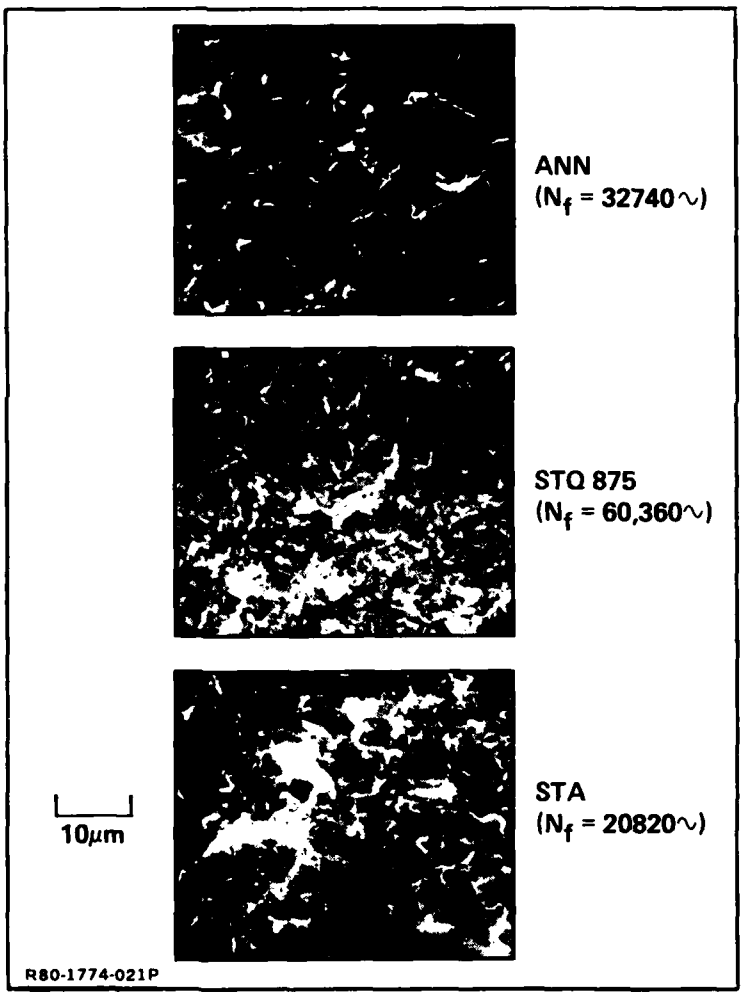

Figure 20. Fracture surfaces near initiation site in heat treated 9.5 mm Ti-6Al-4V rod (strain = ±0.007).

3.3 TENSILE PROPERTIES AND HARDNESS

The tensile and hardness properties of selected heat treat conditions for the Ti-6Al-4V materials in this work are shown in Tables 8 and 9. It can be seen that the yield strengths of the STQ conditions in practically all cases were lower than the yield strengths of the corresponding ANN conditions. Similarly, the ultimate strengths of the STQ conditions were always higher than the annealed conditions. A measure of the relatively high strain hardening rate of the STQ conditions is shown in both the true strain at maximum load, ε_u (which is an approximation of the strain hardening exponent) and the ratio of ultimate to yield strength, $\frac{UTS}{YS}$. Typically, the STQ conditions are characterized by high values of ε_u ($\geq$ 10%) and UTS/YS ($\geq$ 1.2). These values were quite similar and consistent for each of the materials tested.

Young's modulus, E, was determined graphically for each condition. The E values tend to be lower than usually expected for this Ti-6Al-4V, which in part is attributed to a possible texturing effect of the rods. A reduction in the elastic modulus as a result of solution treating is a characteristic that has also been observed elsewhere (Ref. 11). The formation of martensite during quenching apparently lowers E, but aging raises it again, as can be seen in the values for the STA condition.

The lower hardness values of some of the STQ conditions listed in Table 9 compared to the ANN conditions seems to be inconsistent when considering the higher ultimate strengths of the STQ conditions. This is attributed to the high work hardening capacities of the solution treated conditions, which are not fully exhausted during hardness testing. This effect has also been observed in other Ti-6Al-4V heat treat conditions (Ref. 12).

3.4 CYCLIC DEFORMATION CHARACTERISTICS

A number of typical plots comparing stress range as a function of applied fatigue cycles for the ANN, STA, and STQ 900 conditions in three heats of Ti-6Al-4V is shown in Figures 21 to 23, respectively. These plots were derived from measurements of hysteresis loops obtained at various stages during the fatigue life of each heat treat condition during constant strain cycling. It can be seen that all conditions underwent cyclic softening during their lifetimes.

TABLE 8. SUMMARY OF TENSILE PROPERTIES FOR Ti-6Al-4V HEAT TREATED MATERIAL.

Ti-6Al-4V MATERIAL	HEAT TREAT CONDITION	YIELD STRENGTH, YS 0.2 PERCENT MPa (KSI)	ULTIMATE STRENGTH, UTS MPa (KSI)	MODULUS, E GPa (PSI, 10^6)	TRUE STRAIN AT MAXIMUM LOAD, ϵ_u, %	TOTAL ELONGATION, %	$UTS/_{YS}$
9.5 mm, ROD, CODE D	ANN	952 (138)	1041 (151)	106.9 (15.5)	8.8	20	1.09
	STA	1138 (165)	1213 (176)	113.1 (16.4)	6.0	16	1.07
	STQ 875 (1)	896 (130)	1089 (158)	100.7 (14.6)	10.3	26 (3)	1.22
6.4 mm, ROD, CODE K	ANN	1027 (149)	1069 (155)	95.8 (13.9)	6.8	15	1.04
	STA	1172 (170)	1255 (182)	107.6 (15.6)	4.9	13	1.07
	STQ 850	793 (115)	1096 (159)	90.3 (13.1)	10.4	19	1.38
	STQ 875	848 (123)	1096 (159)	90.3 (13.1)	10.7	21	1.29
	STQ 900	945 (137)	1151 (167)	95.2 (13.8)	10.7	18	1.22
	STQ 925 (1)	1089 (158)	1241 (180)	102.0 (14.8)	7.2	13 (3)	1.14
3.2 mm, SHEET CODE P	ANN	958 (139)	1000 (145)	109.0 (15.8)	8.3	15	1.04
	STA	1069 (155)	1145 (166)	115.1 (16.7)	7.2	14	1.07
	STQ 875 (2)	780 (116)	1048 (152)	95.8 (13.9)	11.3	20 (4)	1.31

(1) Average of Two Tests
(2) Average of Three Tests
(3) % Elongation in 0.500 in. gage
(4) % Elongation in 1.00 in. gage

R80-1774-039(T)

TABLE 9. HARDNESS OF Ti-6Al-4V HEAT TREAT CONDITIONS.

HEAT TREAT CONDITION	MICROHARDNESS, KNOOP (500g)*				
	12.7 mm ROD (CODE A)	12.7 mm ROD (CODE B)	9.5 mm ROD (CODE D)	6.4 mm ROD (CODE K)	3.2 mm SHEET (CODE P)
ANN	332 ± 8	311 ± 7	331 ± 20	302 ± 4	309 ± 9
STA	335 ± 10	355 ± 9	362 ± 21	344 ± 3	360 ± 11
STQ 825	–	–	–	–	283 ± 39
STQ 850	309 ± 5	307 ± 10	307 ± 5	283 ± 7	315 ± 7
STQ 875	336 ± 6	318 ± 8	309 ± 18	300 ± 3	321 ± 9
STQ 900	350 ± 6	369 ± 28	361 ± 26	274 ± 8	333 ± 11
STQ 925	386 ± 26	356 ± 10	366 ± 16	354 ± 3	366 ± 8
BQ 1040	398 ± 42	352 ± 6	380 ± 11	–	–

* Average of 5 Readings

R80-1774-040(T)

Each corresponding heat treat condition, for example the $\alpha + \beta$ annealed (ANN) condition in Figure 21, exhibited similar rates of cyclic softening. This similarity was consistently observed for all the other heat treat conditions, including the STQ conditions not shown. In all heats of Ti-6Al-4V, the ANN and STA condi-

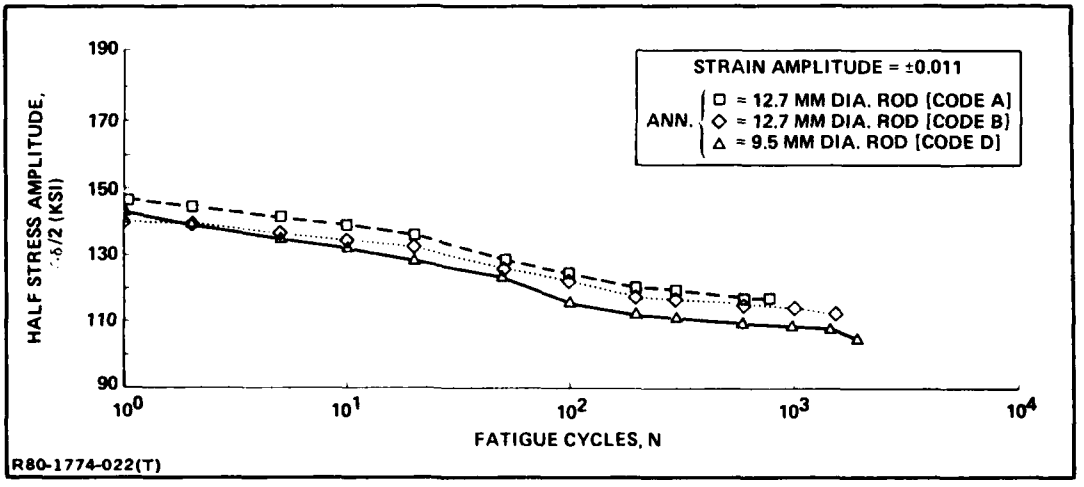

Figure 21. Comparison of stress variations during constant strain cycling of Ti-6Al-4V in annealed condition.

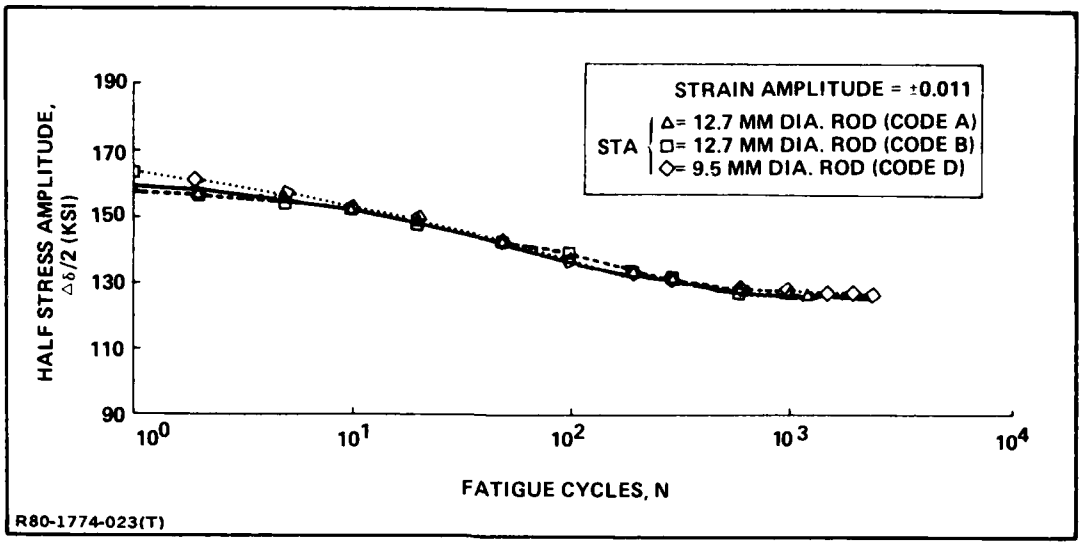

Figure 22. Comparison of stress variations during constant strain cycling of Ti-6Al-4V in STA condition.

tions had generally higher softening rates than the STQ conditions. A comparison of cyclic stress variations for the STQ conditions of the 9.5 mm rod is shown in Figure 24. The STQ 850 and STQ 875 conditions exhibited lower rates of softening during early stage fatigue.

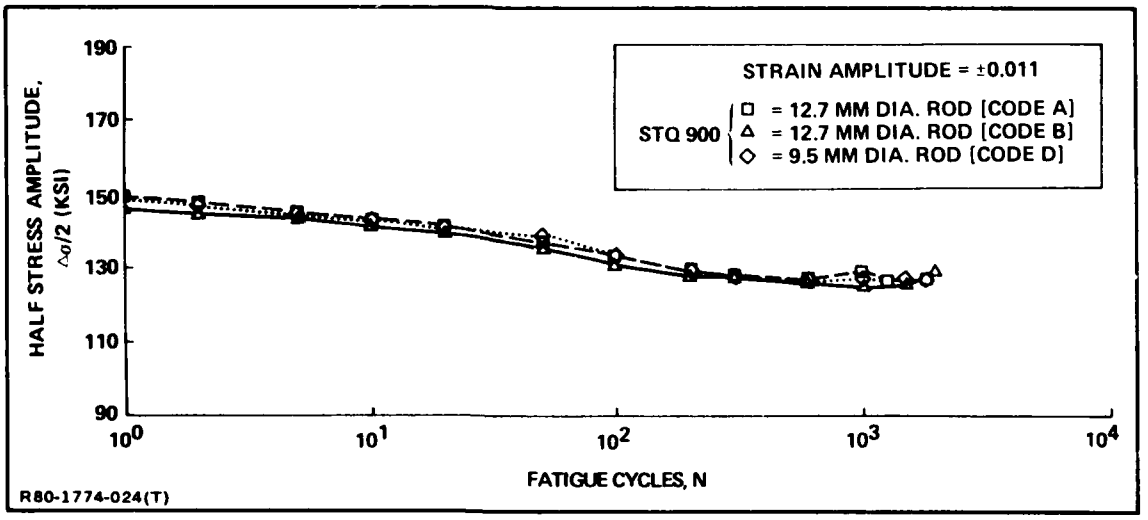

Figure 23. Comparison of stress varistions during constant strain cycling of Ti-6Al-4V in STQ 900 condition.

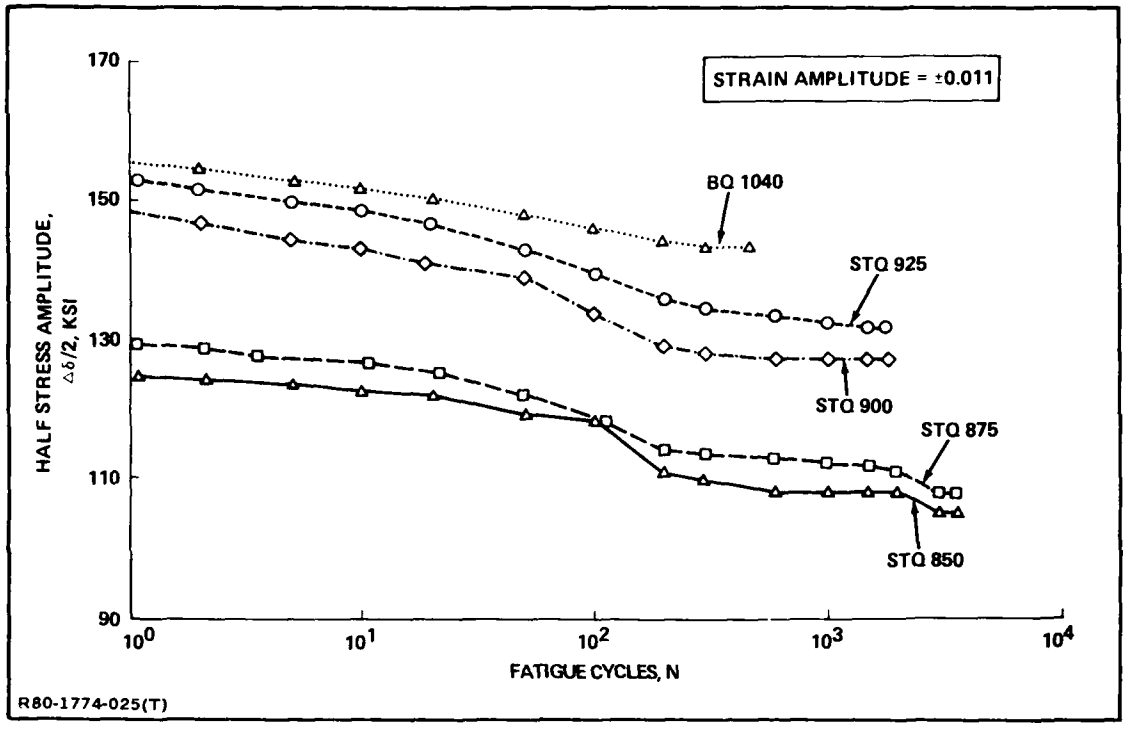

Figure 24. Variation in stress during constant strain cycling of water quenched Ti-6Al-4V rod - 9.5 mm diameter (Code D).

A comparison of cyclic stress variations for the ANN, STA, and STQ 875 conditions of the 9.5 mm rod is shown as a function of fatigue cycles and percent lifetime in Figures 25 and 26, respectively. The rate of softening of the STQ 875 condition is considerably less than the other conditions and, in fact, exhibits relatively little change within the early stages, as shown in Figure 25. Comparing the half-life stresses, the STQ 875 condition softened only about one-half as much as the ANN and STA conditions, as seen in Figure 26. The greatest changes in stress occurred within the first 10 percent of lifetime for each condition. The STQ 875 condition underwent less change in stress and reached an apparent steady state stress in less than 10 percent of its lifetime.

An indication of the relatively higher cyclic stability of the STQ 875 condition is also seen by comparing the UTS/YS ratios and ε_u values in Table 8. The UTS/YS ratios for the ANN, STA, and STQ 875 conditions of the 9.5 mm rod are 1.09, 1.07, and 1.22, respectively; the ε_u values are 0.088, 0.06, and 0.103, respectively. It has been found generally that metals with UTS/YS ratios $\geq$ 1.4

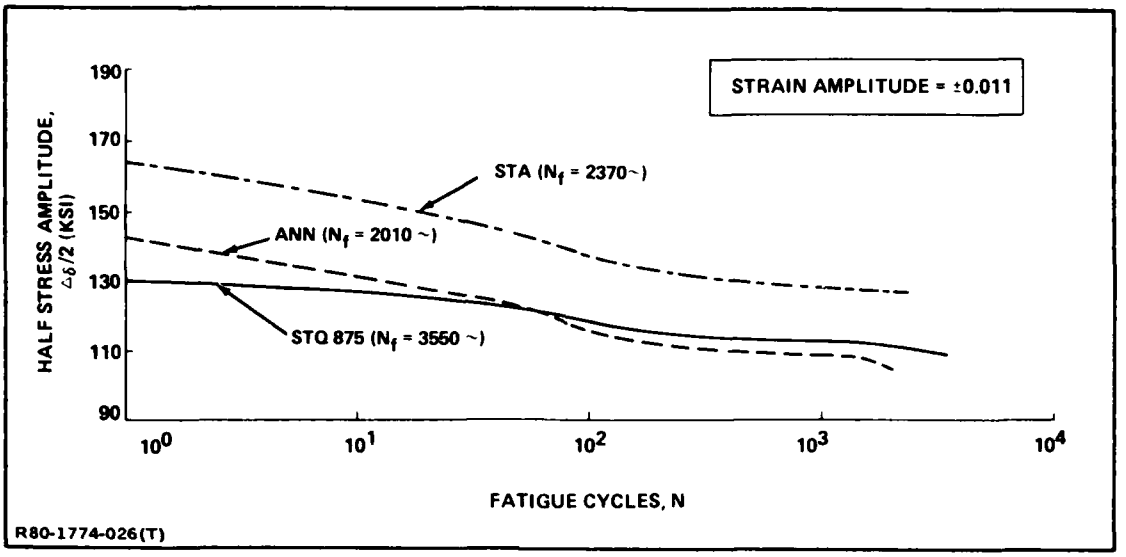

Figure 25. Variation in stress during constant strain cycling of Ti-6Al-4V rod – 9.5 mm diameter (Code D).

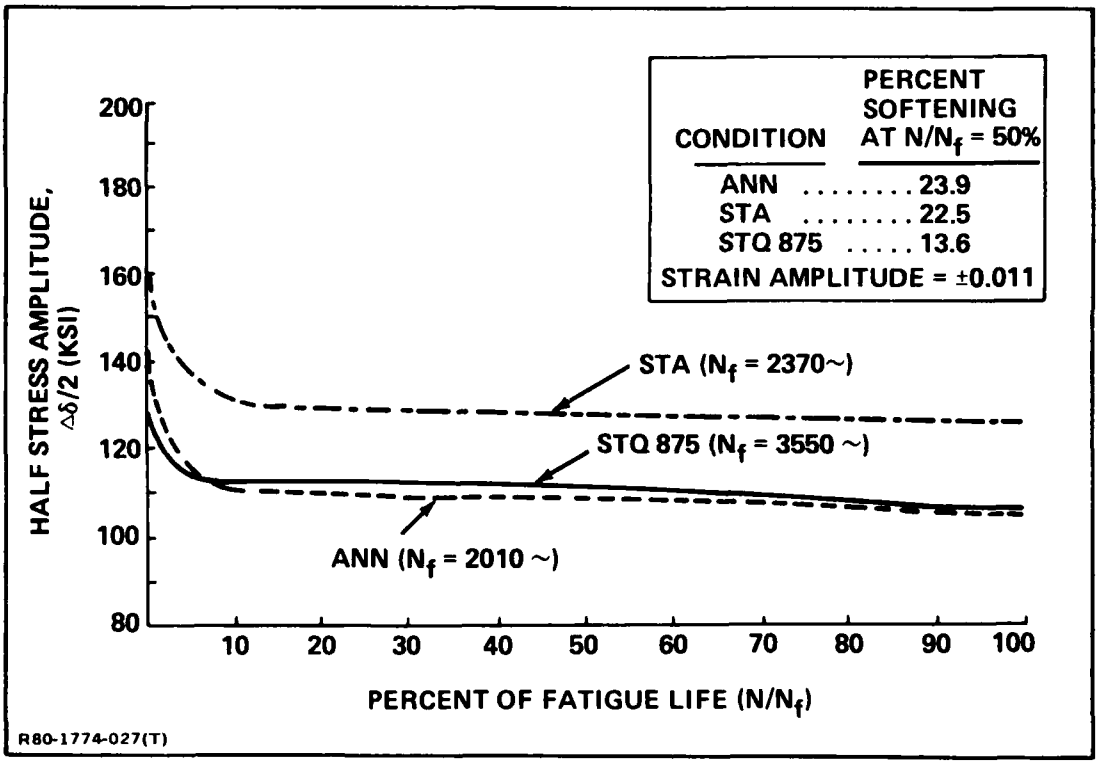

Figure 26. Variation in stress range during constant strain cycling of three heat treat conditions in Ti-6Al-4V rod – 9.5 mm diameter (Code D).

(higher ε_u) cyclically harden while those with values ≤ 1.2 cyclically soften (low ε_u) (Ref. 13). Thus, the higher apparent cyclic stability of the STQ 875 condition is reflected in its higher UTS/YS ratio. This characteristic was observed for the other STQ conditions tested in this work.

3.5 FATIGUE CRACK INITIATION

A relative measure of fatigue crack initiation resistance for various heat treat conditions in the 3.2 mm sheet, center-hole notched specimens, was determined using acoustic emission (AE). In this work, crack initiation lifetime is defined as the number of fatigue cycles necessary to attain a total of 100 acoustic emission events, where an "event" is usually associated with the formation of some form of microcracking in the test specimen. The criterion of 100 acoustic events was empirically determined and is based on our scanning electron microscopic observations of micron-sized cracks which result during early stage fatigue. Thus, a specimen exhibiting a relatively high rate of event accumulation will have a shorter initiation lifetime.

An example of early stage cracking in the 3.2 mm sheet material heat treated to the STQ 875 condition is shown by the SEM fractograph in Figure 27. During early stage fatigue of the center-hole specimens, cracks initiated either at the edges or on the bore surface of the hole. The cracks shown in Figure 27 occurred on the bore surface of the hole, and were present after 100 fatigue cycles, which represents approximately 8 percent of the average of total life of the STQ 875 condition at a maximum stress of 965.3 MPa (140 Ksi). It can be seen that cracking in this case appears to be intergranular, with the crack segments approximating the α particle size of the material. Several specimens were examined in this manner in order to determine a qualitative relationship between AE activity and the relative extent of cracking. No attempt was made to count microcracks and quantitatively correlate them with AE events on a one-to-one basis. Instead, a general relationship was established in which a high rate of AE events indicated a relatively higher incidence of fatigue microcracks.

A comparison of the AE activity in the ANN, STA, and STQ 875 conditions of the 3.2 mm sheet is shown in Figure 28. The AE activity for the STQ 875 condition was relatively low. It required approximately 25 percent of lifetime

to accumulate 100 AE events, compared to 13 percent and 7 percent for the ANN and STA condition, respectively. Typical crack formations in each of these conditions after 100 AE events is shown in Figure 29. The ANN condition contained a high number of relatively large cracks. In comparison, the STQ 875 condition contained a smaller number of cracks than both the ANN and the STA conditions. The apparent average crack size in the STQ 875 condition was intermediate between the other two conditions. Although the STA condition appeared to have a relatively higher number of cracks, they were consistently smaller than any of the other conditions.

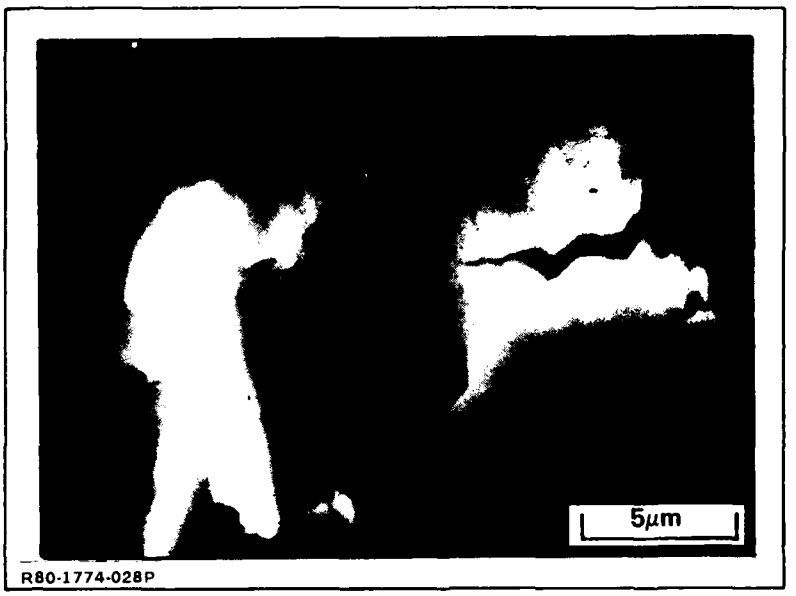

Figure 27. Early stage cracking in 3.2 mm Ti-6Al-4V sheet heat treated in STQ 875.

A comparison of crack initiation life based on AE and overall total lifetimes for all STQ conditions is shown in Figure 30. It can be seen that the average "AE" initiation life is higher for most of the STQ conditions. There is no apparent correlation between initiation lifetime and total lifetime for these specimens. Total lifetime of the STQ conditions steadily increases with ST temperature, while initiation times decrease at higher ST temperatures. The longest times were associated with the STQ 850 and 875 conditions. Although the STA condition appears to have a lower initiation life than the STQ 875 condition, it had the

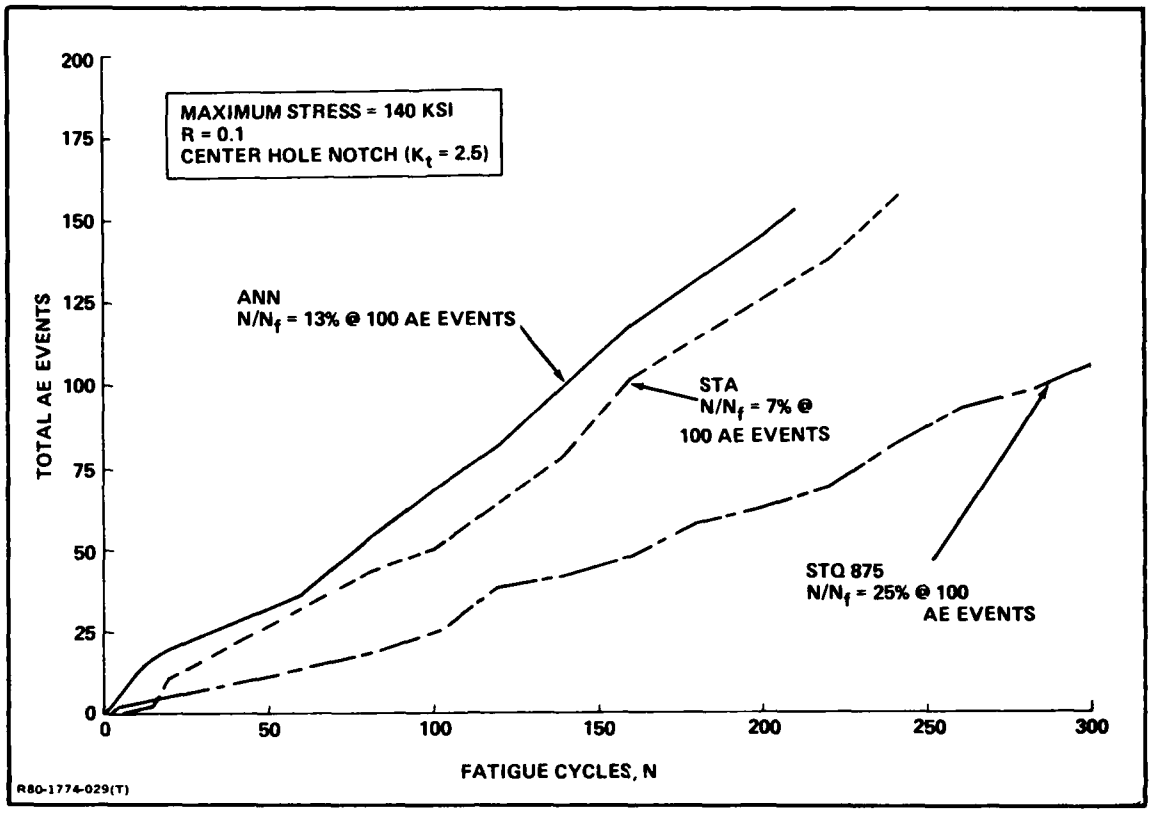

Figure 28. Comparison of acoustic emission in heat treated Ti-6Al-4V sheet (3.2 mm - Code P) during early stage fatigue.

longest lifetime of all the heat treats. A comparison of early stage crack initiation time to total lifetime (i.e., N_i/N_f) for the various conditions tested is shown in Table 10. It can be seen that N_i/N_f for the STQ 825, 850 and 875 conditions were relatively high.

Although the apparent discrepancy between initiation life and total life suggests that the relative crack initiation resistance of a certain condition may be better than its crack propagation resistance, a possible explanation of these results may be related to a notch effect. Since these specimens were tested under constant amplitude load control, the relative notch strains for each condition would be expected to vary depending upon yield strength. The yield

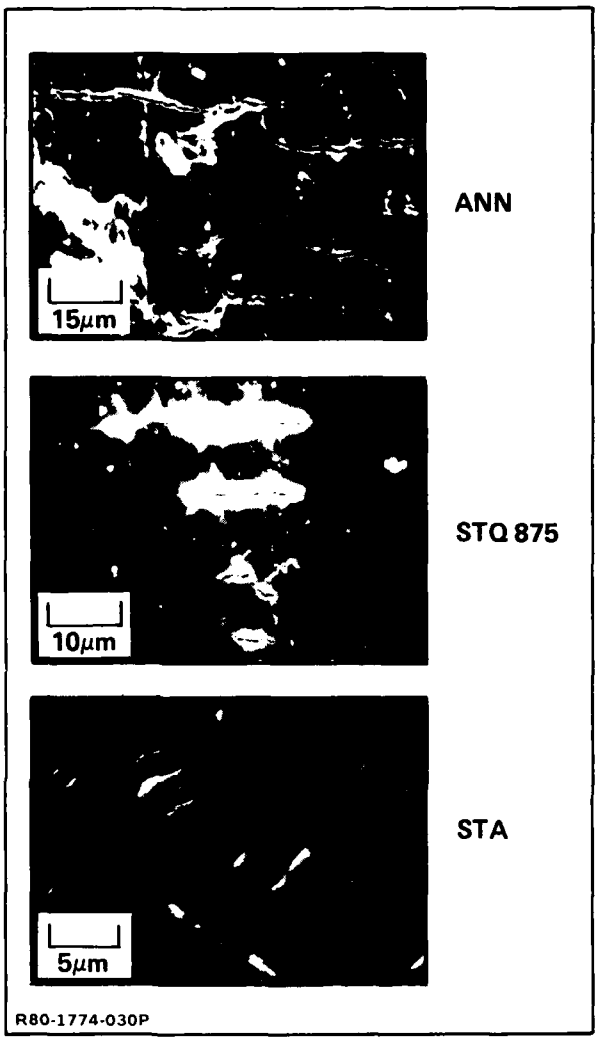

Figure 29. Typical crack formations in notch surfaces of heat treated 3.2 mm Ti-6Al-4V sheet.

strength of the STQ 875 condition in the 3.2 mm sheet is considerably lower than the ANN or STA conditions, as shown in Table 8. At constant load cycling, the relative notch strain of the STQ 875 condition would be quite high compared to the other conditions, and thus, represents a more severe loading condition.

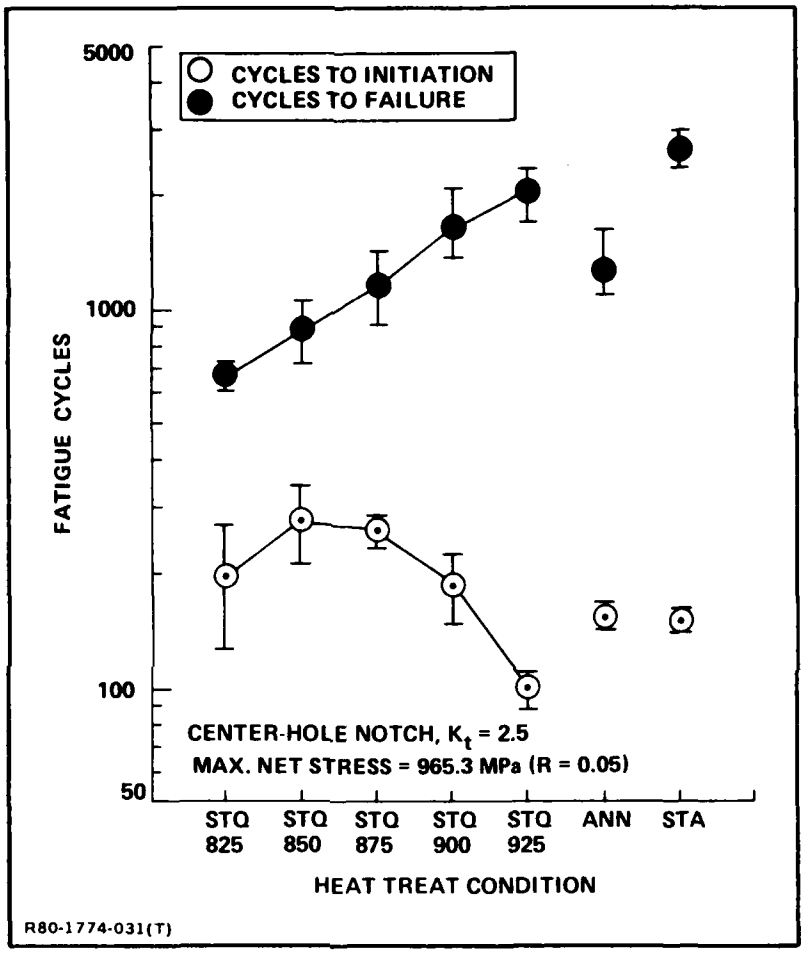

Figure 30. Comparison of fatigue initiation life and total life in Ti-6Al-4V (Code P), 3.2 mm sheet.

TABLE 10. COMPARISON OF EARLY STAGE CRACK INITIATION TO TOTAL FATIGUE LIFETIME (N_i/N_f) IN Ti-6Al-4V SHEET BASED ON ACOUSTIC EMISSION.

HEAT TREAT CONDITION	FATIGUE CYCLES (N_i) / 100 AE EVENTS	FATIGUE LIFE (N_f), CYCLES	N_i/N_f
STQ 825	199	675	.30
STQ 850	280	875	.32
STQ 875	260	1185	.22
STQ 900	188	1672	.11
STQ 925	100	2088	.05
STA	151	2670	.06
ANN	155	1299	.12

Note: Average of 2 Tests.

R80-1774-041(T)

4 - DISCUSSION

The test results for the Ti-6Al-4V heats in this study show that for each material, a particular solution treated and quenched condition produced a distinct improvement in fatigue resistance compared to the annealed condition. Although the microstructural characteristics responsible for the fatigue improvement have not been directly identified in this work, prior studies strongly indicate that strain induced transformation of retained β may be the primary operating mechanism. Thus, the general effects of solution treating and the metastability of β phase are important considerations in explaining the mechanism. Based on the fatigue results in this study and related prior work, it appears that the STQ treatments enhance fatigue life by improving fatigue crack initiation resistance. All of the points above will be included in the following discussion.

4.1 GENERALITY OF HEAT TREATMENT RESPONSE

We have seen from the results in this work that the heat treatment response and behavior of these Ti-6Al-4V heats was very similar. Microstructurally, the optimum STQ conditions are characterized by fine primary α sizes (3 to 5 μm) having an average volume fraction of approximately 0.64, and transformed regions, with closely spaced α' particles ($\leq$0.5 μm). The hardness of similar heat treat conditions were fairly close in most cases. Typically, the hardness of the STQ condition increased with the ST temperature. The tensile and fatigue behavior of the materials tested were also similar. The optimum STQ conditions were characterized by low yield strengths, low moduli, high uniform and total strains, and high strain hardening rates, typified by the UTS/YS ratios. For each rod material, there were at least two STQ conditions with improved fatigue life compared to the ANN conditions. In the sheet material, two STQ conditions exhibited increased crack initiation resistance. Thus, we can see general characteristic behavior between these materials.

Except for fatigue behavior, which has not been studied extensively in solution treated and quenched alloys, many of the above characteristics have been previously observed in Ti-6Al-4V and other α - β titanium alloys that were solution treated and quenched (Refs. 6, 11, 14). For example, in Ti-6Al-6V-2Sn and Ti-8Al-1Mo-1V the UTS/YS ratios for STQ conditions were 2 and 1.25, respectively; hardnesses, yield strengths, and moduli were low (Ref. 14). Fopiano (Ref. 14) showed that Ti-8Al-1Mo-1V in the STQ 927 condition, had superior precracked Charpy toughness compared to other STQ or STA conditions of the same material; no fatigue data were reported. The effect of solution treating and quenching on the tensile and fatigue properties of Ti-6Al-4V bar was studied by Bartlo (Ref. 15). In that work, the STQ 950 condition exhibited a maximum in endurance ratio (fatigue strength/UTS) compared to other STQ conditions, during rotating beam fatigue tests. In both of the above references (14, 15), there was no discussion of the factors which may have been associated with the improved STQ conditions. The minimal interest shown in the properties of solution treated and quenched titanium over the years is not surprising, since it has mainly been considered an intermediate step in producing higher strength aged material.

4.2 STRAIN TRANSFORMATION EFFECTS

It appears that the improved fatigue life of the solution treated and quenched Ti-6Al-4V material tested in this work is primarily due to strain induced shear transformation of retained β to α' as observed by Gilmore (Ref. 4). There is no indication from any previous work that titanium martensites are susceptible to strain induced transformations, such that $\alpha' \rightarrow \beta + \alpha$. Although this possibility exists, it seems less likely since the decomposition of α' is known to be mainly diffusion controlled. It is recognized in titanium that the β phase, produced with just sufficient stabilizing content to retain β by quenching, will form martensite as a result of straining (Refs. 6 to 8, 16, 17). Alloys exhibiting a strain transformation effect typically display low yield stress, uniform elongation, and high strain hardening rates, which are considered properties all useful in metal forming operations. These characteristics were consistently displayed by the materials in this study. This behavior in titanium is analogous to TRIP (transformation induced plasticity) steels in which

deformation induced transformation of retained austenite to martensite leads to high work hardening rates and high elongations (Ref. 18).

4.3 METASTABILITY OF β PHASE

Solution treatment curves for Ti 6/4 typically show a minimum in yield strength at about 840°C, where the vanadium content of the β phase is estimated to be 15 w/o (Ref. 19). According to Jaffee (Ref. 6), this is the approximate minimum vanadium content necessary to retain beta. However, it is apparent from past research on Ti 6/4 that the amount and composition of retained β which can be produced in a given alloy, for a particular solution treatment temperature is a variable, not easily predictable or detectable (Ref. 3, 7, 9, 11, 20 to 22). Specifically, Gilmore (Ref. 3) and Willims (Ref. 7) have reported the presence of primary α, hexagonal martensite, as well as retained β as a result of solution treating 900°C, which is in conflict with the results of others such as Fopiano (Ref. 11). In Fopiano's work, STQ 900 material contained only primary α and α' martensite; β was retained at ST temperatures $\leq$810 C.

It has been shown that aluminum can effectively reduce the amount of β stabilizer needed to retain β on quenching (Ref. 6). Jones (Ref. 17) observed that the deformation stability of the β phase was reduced by decreasing the V/Al content ratio. A comparison of microchemical analysis of the Gilmore (Ref. 3) and Fopiano (Ref. 11) Ti-6Al-4V alloys in the STQ900 condition is shown in Table 11. It can be seen that the α' + β region studied by Gilmore is three times richer in aluminum than the α' region analyzed in the Fopiano work. These differences in aluminum contents raise a question as to how aluminum may affect the metastability of β. The higher aluminum concentration in the Gilmore material may be associated with the retained β that was observed. No conclusions can be reached regarding the effect of chemical composition for the materials in this program. As can be seen in Table 1 there were no large compositional differences between these materials.

Furthermore, the effect of overall compositional variations in Ti 6/4 alloys on the β transus must also be considered in regard to the size, distribution, and microchemistry of β produced during solution treating. For example, a

one w/o decrease in aluminum or one w/o increase in vanadium could lower the β transus in Ti 6/4 approximately 17°C (Ref. 23). Therefore, it is expected that an optimized solution treatment for one material (e.g., STQ 900) may not produce the same effect in another.

TABLE 11. MICROCHEMISTRY OF SOLUTION TREATED AND QUENCHED Ti-6Al-4V.

PHASES OBSERVED	PHASE COMPOSITION		REFERENCES
	Al w/o	V w/o	
α	7.5	2.5	Gilmore (3)
(α' + β)	5.8	6.7	
α	9	2.5	Fopiano (11)
α'	2	6.5	

R80-1774-042(T)

4.4 EFFECTS OF SOLUTION TREATING

In observing the effect of solution treating temperature on hardness, Fopiano (Ref. 11) found that hardness increased with ST temperature, from 840 to 950°C. It was concluded that the hardness increase, without accompanying ductility loss, was attributed to partial aging of the martensite immediately after its formation during the water quench and that the formation of martensite is not a strengthening mechanism in this alloy. The hardness of solution treated Ti 6/4 in the present work showed the same trend of increasing hardness with ST temperature. It was suggested by Fopiano that in the early stages of martensite decomposition, β precipitate was probably present, but its small size hindered detection. Therefore, a certain amount of β may be present in ST material as a result of an initial spontaneous aging reaction, in addition to possible amounts of retained β. If so, the solution treating temperature will strongly influence the size, distribution, and metastability of this constituent.

In the present work, the extent of spontaneous aging during the quench increased with increasing ST temperature, as can be seen in the tensile data for the 6.4 mm rod (CODE K) in Table 8. Since the Ms temperature increases with ST temperature, the aging of martensite during the quench should proceed further at higher ST temperatures, resulting in harder and stronger materials (Ref. 11). The high hardnesses of the βQ 1040 condition, shown in Table 9, are probably the result of extensive autotempering of martensite and finely spaced acicular microstructures.

The high strength and hardness of the STA conditions result from thermally aided spontaneous aging of α' to $\beta + \alpha$. Although β was present in the STA conditions there was no apparent strain induced effect during tensile testing. Similarly, in the ANN conditions, although β was present there were no noticeable transformation effects. The absence of a strain induced effect in these cases is attributed to highly stable β phase, which is not susceptible to deformation. In comparable work on modified Transage 129 alloys, Jones observed true TRIP behavior when the material was tensile strained in the β-annealed condition (Ref. 17). However, when the material was tested in the STA condition there was a complete absence of strain induced effects. He concluded that both conditions depended upon the same strengthening mechanism ($\beta \rightarrow \alpha' + \beta$) and either high yield strength or TRIP behavior could be obtained, but never both simultaneously. The results of the present work appear analogous. The STQ treatments result in low yield strength material, capable of TRIP behavior; thermal aging eliminates the effect. It is not known whether the STQ treatments can be further optimized to increase yield strength and still maintain the strain induced behavior.

4.5 CRACK INITIATION AND GROWTH

The results of this study suggest that optimum STQ conditions enhance early stage crack initiation resistance in both low and high cycle fatigue.

In $\alpha + \beta$ titanium alloys, conflicting requirements appear to exist for fatigue crack initiation resistance and crack propagation resistance (Ref. 4). Generally, very small α grain size and a minimum amount of transformation product improve initiation resistance. Small α grain sizes inhibit twin boundary and slipless

cracking and reduce mean free slip path. Small amounts of transformed β reduce the number, size, and continuity of α + β interfaces. Conversely, improved fatigue crack propagation (FCP) resistance appears to require a maximum amount of β transformation product, characterized by acicular appearing or Widmanstatten microstructures (Refs. 12, 26). Cracking and fracture are often strongly influenced by α + β interfaces and by α layers at prior grain boundaries. Paton, et al (Ref. 25), concluded that the best overall microstructure for strength, toughness, resistance to crack growth, and environmental effects may be the recrystallized annealed (RA) structure.

Improved early stage crack initiation resistance is suggested by the fatigue data presented in Figures 11 to 13. In each case, the fatigue life of the βQ conditions were extremely low. For example, the fatigue lifetimes of the STQ 875 and STA conditions in the 9.5 mm rod, were 7.5 and 5 times greater than the βQ condition. In prior work on crack growth resistance in Ti-6Al-4V it has been observed the βQ microstructures exhibit the best FCP resistance, compared to other conditions, including the primary α -tempered α' microstructure typical of STA (Refs. 12, 26). Since it is well known that in low cycle fatigue, crack initiation life (N_i) is relatively short and most of the lifetime is spent in propagation (N_p), it appears that both the STQ and STA conditions have a greater N_i than the βQ condition, for the alloys in this work. By similar reasoning, the optimum STQ conditions appear to have better initiation resistance than either the ANN or STA conditions.

In another study on the effect of microstructure on notched fatigue properties of Ti 6/4, it was found that superior high cycle fatigue behavior resulted from heat treating above the β transus to produce a fully transformed acicular α structure (Ref. 27). It was suggested that at low stresses the nucleated crack is limited to the width of a single α needle, while at high stresses the nucleated crack may be as large as an entire colony of similarly aligned acicular particles, such as characterized by the βQ conditions in this work.

Improved initiation resistance of solution treated and quenched Ti-6Al-4V is further evidenced by the results of the acoustic emission study on the 3.2 mm sheet and the high cycle fatigue data for the 3/8 in. rod. Although qualitative in nature, the AE data substantiate that early stage cracking proceeds

at a slower rate in STQ material. In this work, the use of notched specimens, fatigued at constant load amplitude, makes the comparison to the smooth bar, constant strain data difficult to interpret. It would be of value to measure the AE characteristics under constant strain conditions in order to discriminate between the N_i and N_p stages.

In earlier work on $\alpha + \beta$ annealed Ti 6/4, Gilmore (Ref. 3) observed that fatigue microcracking initiated in $\alpha + \beta$ phase boundaries, where high strain mismatch would be expected between α grains. In contrast, it was observed that β had been largely eliminated from the α grain boundaries in the STQ 900 condition, where instead, the small α grains ($\simeq 4\mu m$) formed islands within a heavily dislocated β matrix. After straining, α grains appeared dislocation free, and cracks seemed to initiate in transformed α' and avoided α grains (Ref. 28). In his work on STQ conditions, Gilmore measured only total fatigue lifetimes and did not determine crack initiation life.

Generally, fatigue life at stresses near the endurance limit is dominated by N_i. The strain-life data in Figure 18 shows the STQ 875 condition to be superior under high cycle conditions, suggesting that N_i has been enhanced. The role of retained β and strain induced transformation effects on fracture and crack growth in Ti 6/4 have also been considered by others (Refs. 9 and 29). Hall and Hammond suggested that retained β may act as a crack arrestor by producing strain martensite in the plastic zone ahead of a propagating crack (Ref. 9). They noted deviations in the slope of the crack-opening displacement record that were suggestive of such an effect, but they did not consider the evidence conclusive. Benson et al (Ref. 29), on the other hand, considered that a strain induced transformation could represent a structural instability that could lead to accelerated crack growth. However, they found no evidence of strain induced effects and concluded that the β phase was rich enough in vanadium to remain stable under strain.

Based on the results of this study and previous work, it appears that the basic microstructure resulting from the optimum STQ treatments (i.e., presumably primary α, α' martensite and retained β offer relatively more improved resistance of STQ material was demonstrated by the torsional fatigue data of Gilmore, shown in Figure 1. In torsional fatigue, extensive stage I (shear

mode) crack initiation and growth is favored, since the tensile component acting upon the stage I cracks is small (Ref. 30). Thus, cracks continue to grow by stage I mechanism, instead of rapidly changing to stage II (tensile mode), as was the case for the smooth bar, axially strained specimens in this work. Therefore, if N_i was significantly improved, one would expect higher total lifetimes in torsional fatigue over less resistant material. This may account for the order of magnitude improvement of the STQ 900 compared to an ANN data in Figure 1.

4.6 PRACTICAL CONSIDERATIONS AND FUTURE WORK

The results of this work further establish the generality of the heat treatment response of Ti-6Al-4V alloys to solution treating and quenching and, in particular, reinforce the fact that there are specific STQ treatments which possess unique deformation characteristics.

There are many unanswered questions and considerations related to the use of a solution treated and quenched titanium alloy, such as Ti-6Al-4V, in a fatigue critical engineering application. Important engineering properties have not been characterized, such as fracture toughness, FCP, and stress corrosion cracking resistance. In addition, the characteristically low yield strengths and elastic moduli of the STQ condition present a potential limitation if this material is to be strucurally competitive. It is not known if strain susceptible STQ conditions can be further optimized to increase yield strength sufficiently and yet retain the TRIP effect.

The fabricability of STQ material presents some immediate questions on its feasibility and limitations. We don't know the maximum section thickness that can be quenched to condition the materials for strain induced transformation. Quench distortion, residual stress, and dimensional stability of as-quenched parts could be a significant problem. The thermal stability of solution treated and quenched material during and after manufacturing is not known. It is important to establish if the metallurgical improvements offered by STQ treatment will be altered as a result of manufacturing or service environment.

It has not been established if the STQ condition presented in this work could be further optimized, or if there are other heats of Ti-6Al-4V, with

varying thermomechanical histories, that would show greater improvements. In fact, it is quite probable that other $\alpha + \beta$ titanium alloys, such as Ti-6-6-2 or Ti-8-1-1, may offer similar or greater improvements.

It is apparent that many of these questions cannot be sufficiently answered until a clearer understanding of the strain transformation mechanism is obtained. Some of the metallurgical factors that should be addressed in future research include:

1) Effect of prior thermomechanical history and initial microstructural condition.
2) Specific identification of as-quenched products (e.g., type(s) of martensite.
3) Quantitative measurement of volume fractions and structural morphology of phases.
4) Microchemistry of transformation products.
5) Effect of bulk chemical composition.
6) Effect of solution treating holding times and quench rates.
7) Influence of both monotonic and cyclic strain on strain induced transformation and strengthening mechanisms.

5 - CONCLUSIONS

1) Solution treating and water quenching from particular temperatures in the α - β field resulted in improved fatigue resistance of the Ti-6Al-4V materials in this study. Increased low and high cycle fatigue lifetimes under constant axial strain amplitudes were observed compared to α - β annealed and solution treated plus aged conditions.

2) The results of this study suggest that the improvements in fatigue life of the solution treated and quenched condition are manifested by increased resistance to early stage fatigue damage and crack initiation.

3) The improvement in fatigue resistance of solution treated and quenched Ti-6Al-4V appears to be related to strain induced transformation of retained β phase, which results in cyclic energy dissipation instead of fatigue damage accumulation. The specific metallurgical factors to control and optimize the effect of solution treating and quenching have not been determined.

4) The effect of solution treating and quenching on the deformation characteristics of Ti-6Al-4V and other α - β titanium alloys is general (e.g., high ductility and high work hardening rates). Therefore, a strong possibility exists for improved fatigue behavior in this general class of titanium alloys.

6 - REFERENCES

1. Gilmore, C. and Imam, M., "Improvement of Fatigue Properties in Titanium Alloys," Technical Report I (Contract No. N00019-74-C-0086), George Washington University, Washington, D.C., August 1974.

2. Gilmore, C. and Imam, M., "Fatigue Life in Annealed and Martensitic Ti-6Al-4V," Technical Report II (Contract No. N00019-75-C-0093), George Washington University, Washington, D.C., August 1975.

3. Gilmore, C. and Imam, M., "Mechanical Properties of Annealed and Martensitic Ti-6Al-4V," Technical Report III (Contract No. N00019-76-C-0136), George Washington University, Washington, D.C., August 1976.

4. Gilmore, C. and Imam, M., "Mechanical Properties and Microstructure of Heat Treated and Quenched Ti-6Al-4V," Technical Report IV (Contract No. N00019-76-C-0136), George Washington University, Washington, D.C., September 23, 1977.

5. Gilmore, C., Private Communication, July 11, 1977.

6. Jaffee, R.I., "Physical Metallurgy of Titanium Alloys," Progress in Metal Physics, 7, Chalmers, B., ed., Pergamon Press, New York, 1958.

7. Williams, J.C., and Blackburn, M.J., Trans. ASM, 60, p. 373-383, 1967.

8. Jaffee, R.I., "Critical Review - Metallurgical Synthesis," Titanium Science and Technology, Vol. 3, p. 1665, Plenum Press, New York, 1973.

9. Hall, I. and Hammond, C., "Relation Between Crack Propagation Characteristics and Fracture Toughness in $\alpha + \beta$ Titanium Alloys," Titanium Science and Technology, Jaffee, R., ed., Vol. 2, p. 1365, Plenum Press, New York, 1973.

10. Imam, M., Private Communication, February 6, 1979.

11. Fopiano, P., Bever, M., and Averback, B., Trans ASM, 62, p. 324, 1969.

12. Chestnutt, J. et al, "Influence of Metallurgical Factors on the Fatigue Crack Growth Rate in Alpha-Beta Titanium Alloys" Final Report AFML-TR-78-68, Rockwell International Science Center, Thousand Oaks, Calif., May 1978.

13. Landgraf, R., "The Resistance of Metals to Cyclic Deformation," ASTM STP 467, American Society for Testing Materials, p. 3-36, 1970.

14. Fopiano, P., and Hickey, C., "Effect of Heat Treatment on Mechanical Properties of Ti-8Al-1Mo-1V," Titanium Science and Technology, Vol. 2, p. 2009, Plenum Press, New York, 1973.

15. Bartlo, L., "Effect of Microstructure at the Fatigue Properties of Ti 6/4 Bar," ASTM STP 459, p. 144-154, American Society for Testing and Materials, 1969.

16. Crossley, F., et al, "Fracture Toughness of Transage 129 Alloy, Ti-2Al-11V-2Sn-11Zr," Titanium Science and Technology, Vol. 3, p. 2025, Plenum Press, New York, 1973.

17. Jones, R., "Development of Ultrahigh-Strength, Ductile Titanium Alloys By Thermomechanical Processing and Transformation Induced Plasticity," Final Report, Stanford Research Institute, Menlo Park, California, June 1973.

18. Zackay, V., et al, Trans. Amer. Soc. Metals, 60, p. 252, 1967.

19. Wood, R. and Favor, R., Titanium Alloys Handbook, p. 1-4:72-11, (MCIC-HB-02) Metals and Ceramics Center, Bartelle Memorial Institute, December 1972.

20. Averback, B., Comerford, M., and Bever, M., Met. Trans., 215, p. 682, August 1959.

21. Griest, A., Doig, J., and Frost, P., TMS-AIME, 215, p. 627, 1959.

22. Welsch, G. et al, Met. Trans., 8A, p. 169, 1977.

23. Low, C. and Blackburn, M., "Influence of Subsurface Defects on Fatigue Properties of Titanium Alloys," Report EII 75-200-4017B, Pratt & Whitney Aircraft, East Hartford, Connecticut, October 1975.

24. Stubbington, C., "Metallurgical Aspects of Fatigue and Fracture in Titanium Alloys," AGARD Conference Proceedings No. 185, Alloy Design for Fatigue and Fracture Resistance, p. 3-1, April 1975.

25. Paton, N., Williams, J., Chesnutt, J., and Thompson, A., "Effects of Microstructure on the Fatigue and Fracture of Commercial Titanium Alloys," AGARD Conference Proceedings No. 185, Alloy Design for Fatigue and Fracture Resistance, p. 4-1, April 1975.

26. Crossley, F. and Lewis, R., "Correlation of Microstructure With Fracture Toughness Properties In Metals," Final Report LMSC-D356114, Lockheed Research Laboratory, Sunnyvale, Calif., September 1973.

27. Eylon, D. and Pierce, C., Met. Trans., 7A, p. 111, January 1976.

28. Gilmore, C., Private Communication, December 1976.

29. Benson, D., Grosskreutz, J., and Shaw, G., Met. Trans., 3, p. 1239, May 1972.

30. Stubbington, C. and Bowen, A., Jnl. Mat. Sci., 9, p. 947, 1974.

DISTRIBUTION LIST

Department of the Navy
Naval Air Systems Command
Washington, D. C. 20361
Attn: Mr. Michael D. Valentine
AIR-5163C4 (10 copies)
Mr. R. Schmidt
AIR-320A (1 copy)

Department of the Navy
Sea Systems Command
Washington, D. C. 20361
Attn: Code 03423

Chief of Naval Research
Department of the Navy
Washington, D. C. 20361
Attn: ONR 423, 471, (2 copies)

Commander
U.S. Naval Research Laboratory
Washington, D. C. 20390
Attn: Dr. Ray Hettche
Dr. B. B. Rath
Dr. George Yoder

Commanding Officer
Naval Air Development Center,
Johnsville
Aero Materials Laboratory
Warminister, Pennsylvania 18974
Attn: Mr. F. S. Williams

Naval Material Industrial Resources
Office
Philadelphia, PA 19112

Air Force Materials Laboratory
Wright-Patterson Air Force Base
Dayton, Ohio 45433
Attn: Mr. A. M. Adair (LLM);
Dr. H. Lipsett (LLS);
Dr. F. H. Froes

Army Research Office
Box CM, Duke Station
Durham, North Carolina 27706
Attn: Metallurgy and Ceramics Division

United Aircraft Corporation
Sikorsky Aircraft Division
Stratford, CT 06497

Bell Helicopter Company
P. O. Box 482
Forth Worth, TX 76101

National Academy of Sciences
National Materials Advisory Board
2101 Constitution Avenue
Washington, D. C. 20418
Attn: Dr. J. C. Lane

National Aeronautic and Space
Administration
600 Independence Avenue
Washington, D. C. 20546

U.S. Army Materials & Mechanics Research
Center
Watertown Arsenal
Watertown, Massachusetts 02172
Attn: Dr. Saul Isserow

Titanium Metals Corp. of America
400 Rouser Road
P. O. Box 2824
Pittsburgh, PA 15230
Attn: Mr. Larry Mayer

Battelle Memorial Institute
Defense Metals Information Center
505 King Avenue
Columbus, Ohio 43201
Attn: Mr. Richard Wood

Avco Space Systems Division
Lowell Industrial Park
Lowell, Massachusetts 01851

Brush Wellman, Inc.
17876 St. Clair Avenue
Cleveland, Ohio 44110

NASA/Langley
Manufacturing Technology Section
Hampton, VA 23365
Attn: Mr. Tom Bales

The Boeing Company
Aerospace Division
P. O. Box 3707, M/S 73-43
Seattle, Washington 98124
Attn: Mr. Rod Boyer

McDonnell Douglas Research Labs.
St. Louis, Missouri 63166
Attn: Dr. D. P. Ames
Dr. Charles Whitsett

Defense Documentation Center
Cameron Station Bldg. 5
Alexandria, Virginia 22314
Attn: TCA (14 copies)
Via: Naval Air Systems Command
Code AIR-954
Washington, D. C. 20361

The Franklin Institute Research
Laboratories
Twentieth & Parkway
Philadelphia, Pennsyvlania 19103
Attn: Technical Director

Dr. John A. Schey
Department of Mechanical Engr.
University of Waterloo
Waterloo, Ontario
Canada N2L 3G1

Convair Division
General Dynamics
San Diego, California 92112
Attn: Mr. W. Sheck

Dr. Charles Gilmore
School of Engineering and Applied Science
George Washington University
Washington, D. C. 20006

Army Aviation Systems Command
P. O. Box 209
St. Louis, MO 63166
Attn: Mr. R. V. Vollmer (AMSAV-ERE)

AiResearch Co.
Mat'ls Applications Group
93-3G1-503-4V
Attn: Mr. R. G. Berryman
402 S. 36th St.
Phoenix, AZ 85010

ITT Research Institute
10 West 35th Street
Chicago, Illinois 60616
Attn: Dr. N. Parikh

Kawecki Berylco Industries
P. O. Box 1462
Reading, Pennsylvania 19603
Attn: Dr. J. P. Denny

Ladish Company
Packard Avenue
Cudahy, Wisconsin 53110
Attn: Mr. Robert Daykin

Linde Company
Division of Union Carbide
P. O. Box 44
Tonawanda, New York 14152

Lockheed Aircraft Corporation
Lockheed Missile Systems Division
P. O. Box 501 - Orgn. 80-72, Bldg. 18
Sunnyvale, California 91088
Attn: Dr. M. I. Jacobson
Dr. Frank Crossley

Lycoming Division
Avco Corporation
550 South Main Street
Stratford, Connecticut 06497
Attn: Division Library

Midwest Research Institute
425 Volker Boulevard
Kansas City, Missouri 64110

Northrop Corporation
3901 West Broadway
Hawthorne, California 90250
Attn: Mr. Allen Freedman
Dr. Govind Chanani

Solar Division
International Harvester Company
2200 Pacific Highway
San Diego, California 92112
Attn: Dr. A.G. Metcalfe

Wyman Gordon Co.
Attn: Mr. Charles Gure
Worcester Street
North Grafton, MA 05163

United Aircraft Research Laboratory
East Hartford, Connecticut 06108
Attn: Mr. Roy Fanti

Vought Aeronautics Division
LTV Aerospace Corporation
P.O. Box 5907
Dallas, Texas 75222
Attn: Mr. M. McLaren

Dr. Paul Lowenstein
Nuclear Metals, Inc.
2229 Main Street
Concord, Massachusetts 01742

General Electric
Missile & Space Division
Materials Science Section
P.O. Box 8555
Philadelphia, Pennsylvania 91901
Attn: Technical Library

Reynolds Metals Company
Reynold Metals Building
Richmond, Virginia 23218
Attn: Technical Library

Artech Corporation
2816 Fallfax Drive
Falls Church, Virginia 22042
Attn: Mr. Henry Hahn

General Electric Research Laboratory
Schenectady, New York 12301
Attn: Dr. Don Wood

Mr. A. E. Hohman, Jr.
Supervisor, Engineering Materials
Vought Systems Division
LTV Aerospace Corp
P. O. Box 5907
Dallas, TX 75222

Dr. D. H. Peterson
Senior Scientist
Advanced Technology Center, Inc.
P. O. Box 6144
Dallas, TX 75222

Dr. P N. Adler
Plant 26 (Research Dept.)
Grumman Aerospace Corporation
Bethpage, NY 11714

Mr. Carl Micillo
Grumman Aerospace Company
Adv. Mat. & Proc. Division
Bethpage, NY 11714

Aluminum Company of America
1200 Ring Bldg.
Washington, D.C. 20036
Attn: Mr. G.B. Barthold

Pratt & Whitney Aircraft Corp.
400 Main Street
East Hartford, Connecticut 06108
ATTN: Mr. George Rogers
Dr. Alan Lawley
Department of Metallurgical
Engineering
Drexel University
32nd & Chestnut Streets
Philadelphia, Pennsylvania 19104

DISTRIBUTION LIST (Cont)

Dr. Howard Bomberger
Reactive Metals, Inc.
Niles, Ohio 44446

Massachusetts Institute of Technology
Department of Metallurgy and Material Science
Cambridge, Massachusetts 02139
Attn: Dr. N.J. Grant

Mr. Gary Keller
D/115-050, SB04
Rockwell International
Los Angeles International Airport
Los Angeles, CA 90009

Lockheed Aircraft
Attn: Mr. Rod Siemenz
Dept. 74-50, Bldg 85
Burbank, CA 91520

Doublas Aircraft Company
3855 Lakewood Boulevard
Long Beach, CA 90846

Defense Advanced Research Project Agency
1400 Wilson Boulevard
Arlington, Virginia 22209
Attn: Dr. E.C. VanReuth

Dr. Neil Paton
Rockwell International Corp.
Science Center
P.O. Box 1085
1049 Camino Dos Rios
Thousand Oaks, CA 91360

Pratt & Whitney Aircraft
Division of United Aircraft Corp.
Florida Research & Development Center
P.O. Box 2691
West Palm Beach, FL 33402
Attn: Mr. John Miller

McDonnell Aircraft Co.
St. Louis, Missouri 63166
Attn: Mr. H.C. Turner

Dr. J.C. Williams
Department of Metallurgy and Materials Science
Carnegie-Mellon University
Pittsburgh, Pennsylvania 15213

Westinghouse Electric Corporation
Central Research Laboratories
Attn: Dr. Alan T. Male
Manager, Material Processing Research
Beulah Road, Churchill Borough
Pittsburgh, PA 15235

Crucible Materials Research Center
P. O. Box 88
Parkway West and Route 60
Pittsburgh, PA 15230
ATTN: Mr. E. J. Dulis

Loskheed Missiles & Space Company, Inc.
Palo Alto Research Laboratory
3251 Hanover Street
Palo Alto, California 94304
Attn: Dr. Thomas E. Tietz
52-31/204

Titanium Metals Corporation of America
Henderson, Nevada 89015
Attn: Mr. James Hall

Grumman Aerospace Corporation
Bethpage, L.I., New York 11714
Attn: Mr. R. Heitzmann (2 copies)

Mr. George Hsu
Manager of Industry Standards
Reynolds Metals Corp.
6601 W. Broad Street
Richmond, Virginia 23261

Dr. John K. Tien
Henry Krumb School of Mines
Columbia University
New York, New York 10027

Boeing Vertol Company
Boeing Center
P.O. Box 16858
Philadelphia, Pennsylvania 19142


DATE
ILME
8